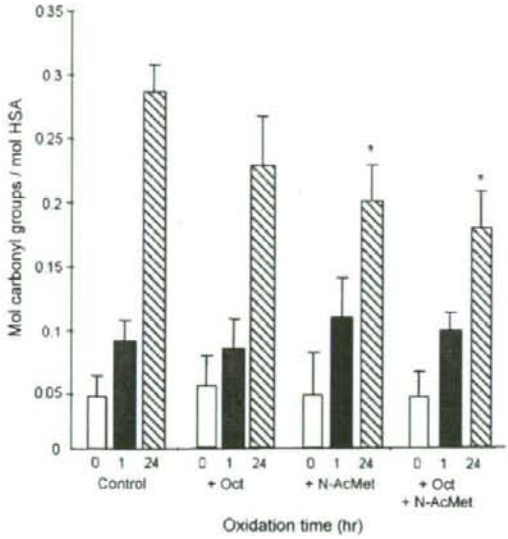

Fig. 1. AAPH-induced oxidation of HSA alone (control) and in the presence of ligands. The values are mean ± S.D. ($n = 4$). $^{*}p < 0.01$ as compared with control.

N-AcTrp, reported previously (Anraku et al., 2004). Protection against oxidation was even more pronounced when both *N*-AcMet and Oct were present; this effect was mainly due to the presence of *N*-AcMet because addition of Oct alone gave no significant protection (Fig. 1).

We also investigated whether AAPH treatment for 1 h affects the status of the SH group of 34-Cys using quantitative analysis of chromatograms given in Table 1 and Fig. 2. Exposure to AAPH resulted in a pronounced reduction in the amount of HMA, the relative area of the peak decreased from 65.1% to 22.3%, showing that AAPH was also capable of oxidizing SH groups of Cys residues. This hypothesis was supported by a calculation of peak areas (Table 1). N-AcMet had a protective effect in the presence or absence of Oct. Quantitative analysis presented in Table 1 shows that this effect was significant for *N*-AcMet, as well as for *N*-AcTrp (Anraku et al., 2004).

Table 1
Relative fractions of HMA, HNA-1 and HNA-2 (%) before and after oxidation by AAPH[a]

	HSA alone	+Oct	+*N*-AcMet	+Oct + *N*-AcMet
Before oxidation				
HMA	65.1 ± 2.3	66.1 ± 2.9	65.3 ± 2.5	65.3 ± 2.5
HNA-1	22.8 ± 2.5	23.4 ± 4.2	21.5 ± 3.5	22.5 ± 3.7
HNA-2	10.6 ± 5.3	10.8 ± 4.5	11.6 ± 4.5	11.5 ± 5.4
After oxidation				
HMA	22.3 ± 2.8	22.3 ± 2.5	39.3 ± 2.3*	39.2 ± 2.6*
HNA-1	51.4 ± 2.5	51.3 ± 4.2	46.3 ± 3.2*	45.6 ± 3.4*
HNA-2	26.7 ± 5.3	26.5 ± 4.5	12.4 ± 4.5*	15.5 ± 5.5*

[a] The concentration of HSA was 50 μM, and that of AAPH and the ligands was 10 mM and 250 μM, respectively. The results are average values ± S.D. for three experiments.
* $p < 0.05$ as compared with HSA alone.

3.2. Scavenging of DPPH radicals in solution

The effects of *N*-AcMet and *N*-AcTrp were examined by monitoring the change in the absorbance of DPPH radicals during 15-min incubation. As shown in Fig. 3, HSA with *N*-AcMet

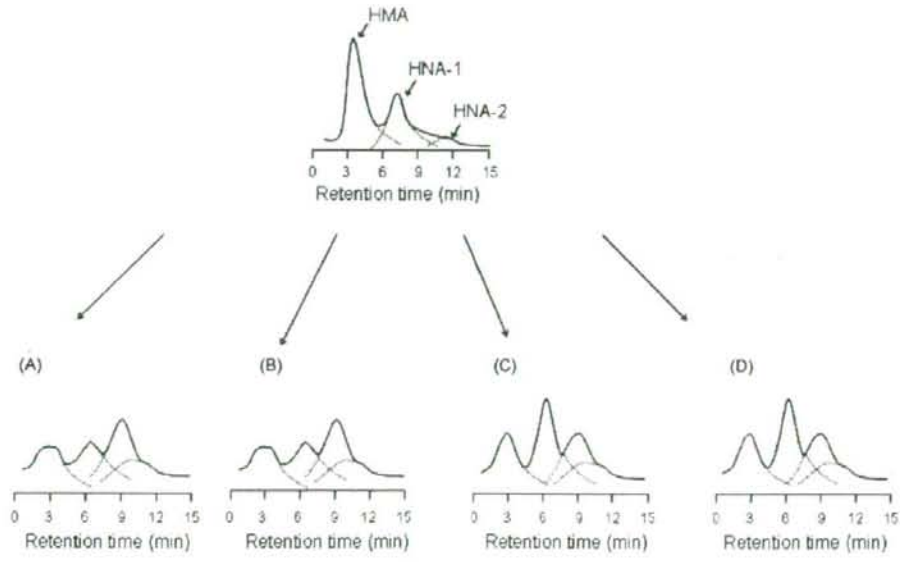

Fig. 2. HPLC chromotograms of HSA before (upper curves) and after AAPH-induced oxidation (lower curves). (A) Oxidation of albumin in absence of additives, (B) oxidation in the presence of Oct, (C) oxidation in the presence of *N*-AcMet, (D) oxidation in the presence of *N*-AcMet and Oct. Peaks correspond to HMA, HNA-1 and HNA-2. Data shown are from representative experiments.

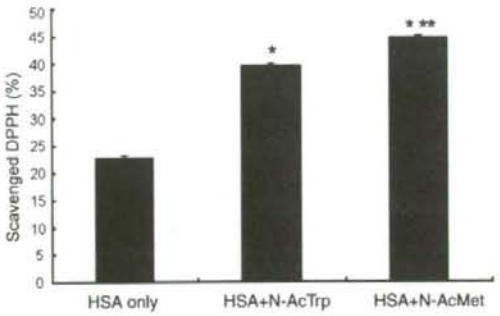

Fig. 3. Radical scavenging ability of HSA with ligands. $^{*}p<0.05$, compared with blank. $^{**}p<0.05$, compared with *N*-AcTrp.

and *N*-AcTrp were better scavengers of DPPH radicals than HSA alone. It should be noted that the scavenging ability of *N*-AcMet was higher than that of *N*-AcTrp (*N*-AcTrp; 39.5 ± 0.3, *N*-AcMet; 44.6 ± 0.4, $p<0.05$).

3.3. Effect of heating on HSA in the presence and absence of N-AcMet

The effect of *N*-AcMet on the thermogram of HSA as determined by DSC was examined. For HSA, which had not been preheated, the addition of the ligands shifts the thermogram towards higher temperature as follows (Fig. 4A): Oct + *N*-AcMet > Oct > *N*-AcMet > HSA alone. The results obtained after preheating these samples are shown in Fig. 4B. In this case, no normal thermogram was obtained for HSA alone. However, addition of additives protected albumin during preheating, and these samples resulted in thermograms which were shifted towards higher temperatures in the same as in Fig. 4A. As shown in Table 2, the addition of *N*-AcMet alone produced a slight increase in T_m and an increase in ΔH_{cal} before and after preheating. Further, incubation of HSA with Oct and *N*-AcMet produced a more stable state than HSA alone. The effect of *N*-AcMet was similar to that of *N*-AcTrp (Anraku et al., 2004).

Table 2
Thermodynamic data obtained from DSC of different HSA samples at pH 7.4[a]

Protein samples	T_m (°C)	ΔH_{cal} ($\times 10^2$ kcal/mol)	$\Delta H_v/\Delta H_{cal}$ ($\times 10^2$ kcal/mol)
Without preheating			
HSA	59.50 ± 0.06	1.64 ± 0.11	0.7 ± 0.01
HSA+Oct	66.83 ± 2.10	2.10 ± 0.15	0.7 ± 0.01
HSA + *N*-AcMet	60.06 ± 0.10	1.71 ± 0.05	0.7 ± 0.03
HSA + Oct + *N*-AcMet	66.51 ± 0.15	2.03 ± 0.09	0.7 ± 0.01
With preheating[b]			
HSA	ND[c]	ND	ND
HSA + Oct	66.80 ± 0.04	2.10 ± 0.19	0.7 ± 0.01
HSA + *N*-AcMet	61.58 ± 0.06	0.91 ± 0.25	1.9 ± 0.01
HSA + Oct + *N*-AcMet	66.46 ± 0.05	1.96 ± 0.25	0.8 ± 0.02

[a] The concentration of HSA was 0.1 mM, and that of the ligands was 0.5 mM. The results are average values ± S.D. for three experiments.
[b] Preheating was incubation at 60 °C for 30 min.
[c] No normal thermogram could be detected.

3.4. Thermal stabilities of HSAs in the presence and absence of N-AcMet for clinical application

As a result, in the sample without the addition of the additive, the aggregate of HSA and rHSA by heating were distinctly generated. On the other hand, no contaminant was observed in the two samples with the addition of *N*-AcMet (data not shown).

4. Discussion

For hypoalbuminemia, which is hard to control, albumin preparations are used for supplementation to improve clinical conditions. Specifically, albumin is indispensable for modern medical treatment because they are generally used for collection of a circulating plasma volume in hemorrhagoc and traumatic shock, improvement of edema, and various kinds of diseases such as liver cirrhosis and nephrotic syndrome (Peters, 1996).

Conventionally, the production of HSA involves fractionating blood collected from human sources, and purifying the obtained albumin-containing aqueous solution according to var-

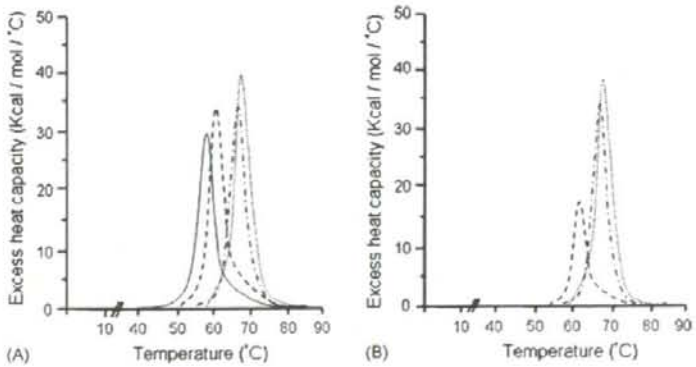

Fig. 4. Effect of Oct and *N*-AcMet on the thermogram of HSA obtained by DSC. (A) Curves for samples that were not preheated. (B) Curves for samples which have been preheated for 30 min at 60 °C. Results are shown for HSA alone (—), HSA with *N*-AcMet (- - -), HSA with Oct (- · - · -), and HSA with both ligands (· · ·). Data are averages of three experiments.

ious purification methods. In the production of HSA, low-temperature pasteurization (60 °C for 10 h) is performed to remove harmful heat-sensitive viruses and to prevent protein contamination is performed. Because the viruses are usually destroyed by heating at 60 °C for several hours without denature of HSA. In low-temperature pasteurization, *N*-AcTrp and Oct are added to HSA as stabilizers (Ballou et al., 1944; Boyer et al., 1946), but *N*-AcTrp has a possible side effect of intracerebral disease (Aguilera et al., 2001). The resulting accumulation of Trp metabolites in nervous tissue may be involved in pathogenesis of several neurological disorders in uremia (Topczewska-Bruns et al., 2003). To provide HSA preparations safely and without risk of side effects, it is important to find new stabilizing reagents instead of *N*-AcTrp.

Moskovitz et al. (1997) recently suggested that oxidation of surface-exposed Met residues to Met sulfoxide is a defense against extensive and irreversible oxidative modification of proteins. Further, Bourdon et al. (2005) suggested that Cys primarily acts as a free radical scavenger, whereas Met primarily acts as a metal chelator on the HSA molecule, although other amino acid residues are likely to be involved in the anti-/prooxidant properties of HSA. Under such circumstances, we focused on *N*-AcMet.

In the present studies, we first compared the protective effect of *N*-AcMet with *N*-AcTrp on oxidation of HSA. HSA was exposed to AAPH, which oxidizes histidine, Trp, tyrosine and Met residues in proteins (Ma et al., 1999; Bourdon et al., 2005). As shown in Fig. 1, the carbonyl content of HSA increased with incubation time. By contrast, *N*-AcMet had a protective effect during prolonged exposure to oxidant, as does *N*-AcTrp (Anraku et al., 2004). In mercaptalbumin (HMA) the last Cys residue, at position 34, has a free SH group. *In vivo*, a major part of the group is either bound to free Cys or glutathione (HNA-1) or is oxidized to sulfenic, sulfinic or sulfonic states (HNA-2). In this study, we also investigated whether AAPH-treatment for 1 hr affects the status of the SH group of 34-Cys. Exposure to AAPH resulted in oxidization of SH-groups of Cys residues (Fig. 2 and Table 1). Incubating Oct together with AAPH has no effect on oxidation. By contrast, the presence of *N*-AcMet has a protective effect, which was the same for the absence (Fig. 2C) or presence (Fig. 2D) of Oct. Thus, with respect to the potential oxidation of HSA, *N*-AcMet, but not Oct, had a significant protective effect. In addition, we found by using DPPH radical that *N*-AcMet produced significant protection against free radicals, compared to *N*-AcTrp (Fig. 3). This suggests that *N*-AcMet is more useful than *N*-AcTrp as a stabilizer.

To validate the benefit of *N*-AcMet as a stabilizer, we also studied the stabilizing effect of *N*-AcMet by DSC. It is seen that the endotherms were single and sharp peaks, indicating that thermal denaturation can be explained by a single component model (Picó, 1997; Anraku et al., 2001). Therefore, single values for T_m, ΔH_{cal} and ΔH_v could be calculated (Table 2). Further, ΔH_{cal}, which is generally thought to reflect the hydration of hydrophobic regions buried in the native protein structure during the unfolding process, varied similarly to the T_m values. The ratio of $\Delta H_v/\Delta H_{cal}$ is an index of the transition process to the denaturation states of proteins during thermal denaturation (Kosa et al., 1998). The values of these ratios for preheated samples with Oct were almost identical to those for unheated samples, whereas those of the *N*-AcMet containing sample increased. Thus, Oct gave a greater protection against heat stress than *N*-AcMet. In our previous work, we have also studied in some detail the effect of *N*-AcTrp on the structural stabilities of HSA. Experiments performed with circular dichronism and native-PAGE showed that Oct and *N*-AcTrp have a pronounced stabilizing effect on the structure of monomeric HSA during heating, as shown by higher T_m- and ΔH_{cal}-values (Anraku et al., 2004). In the case of *N*-AcMet and Oct, we also observed structural stabilities of HSA for these experiments (data not shown).

In recent years, technology for the mass production of albumin with recombinant HSA has been established (Storch, 1993). In the near future, highly stable and inexpensive rHSA stabilized by *N*-AcMet may be available for clinical application.

References

Aguilera, A., Selgas, R., Diez, J.J., Bajo, M.A., Codoceo, R., Alvarez, V., 2001. Anorexia in end-stage renal disease: pathophysiology and treatment. Expert. Opin. Pharmacother. 2, 1825–1838.

Anraku, M., Tsurusaki, Y., Watanabe, H., Maruyama, T., Kragh-Hansen, U., Otagiri, M., 2004. Stabilizing mechanisms in commercial albumin preparations: octanoate and *N*-acetyl-L-tryptophanate protect human serum albumin against heat and oxidative stress. Biochim. Biophys. Acta 1702, 9–17.

Anraku, M., Yamasaki, K., Maruyama, T., Kragh-Hansen, U., Otagiri, M., 2001. Effect of oxidative stress on the structure and function of human serum albumin. Pharm. Res. 18, 632–639.

Arakawa, T., Kita, Y., 2000. Stabilizing effects of caprylate and acetyltryptophanate on heat-induced aggregation of bovine serum albumin. Biochim. Biophys. Acta 1479, 32–36.

Ballou, G.A., Boyer, P.D., Luck, J.M., Lum, F.G., 1944. The heat coagulation of human serum albumin. J. Biol. Chem. 153, 589–605.

Bourdon, E., Loreau, N., Lagrost, L., Blache, D., 2005. Differential effects of cysteine and methionine residues in the antioxidant activity of human serum albumin. Free Radic. Res. 39, 15–20.

Boyer, P.D., Lum, F.G., Ballou, G.A., Luck, J.M., Rice, R.G., 1946. The combination of fatty acids and related compounds with serum albumin. I. Stabilization against heat denaturation. J. Biol. Chem. 162, 181–198.

Brot, N., Weissbach, H., 1983. Biochemistry and physiological role of methionine sulfoxide reductase in proteins. Arch. Biochem. Biophys. 223, 271–281.

Chen, R.F., 1967. Removal of fatty acids from serum albumin by charcoal treatment. J. Biol. Chem. 242, 173–181.

Climent, I., Tsai, L., Levine, R.L., 1989. Derivatization of g-glutamyl semialdehyde residues in oxidized proteins by fluoresceinamine. Anal. Biochem. 182, 226–232.

Kogure, K., Goto, S., Abe, K., Ohiwa, C., Akasu, M., Terada, H., 1999. Potent antiperoxidation activity of the bisbenzylisoquinoline alkaloid cepharanthine: the amine moiety is responsible for its pH-dependent radical scavenge activity. Biochim. Biophys. Acta 1426, 133–142.

Kosa, T., Maruyama, T., Otagiri, M., 1998. Species differences of serum albumins. II. Chemical and thermal stability. Pharm. Res. 15, 449–454.

Ma, Y.S., Chao, C.C., Stadtman, E.R., 1999. Oxidative modification of glutamine synthetase by 2,2′-azobis(2-amidinopropane) dihydrochloride. Arch. Biochem. Biophys. 363, 129–134.

Moskovitz, J., Berlett, B.S., Poston, J.M., Stadtman, E.R., 1997. The yeast peptide-methionine sulfoxide reductase functions as an antioxidant in vivo. Proc. Natl. Acad. Sci. U.S.A. 94, 9585–9589.

Narazaki, R., Harada, K., Sugii, K., Otagiri, M., 1997. Kinetic analysis of the covalent binding of captopril to human serum albumin. J. Pharm. Sci. 86, 215–219.

Niki, E., 1987. Antioxidants in relation to lipid peroxidation. Chem. Phys. Lipids 44, 227–253.

Peters Jr., T., 1996. All about Albumin: Biochemistry, Genetics and Medical Applications. Academic Press, San Diego, CA.

Picó, G.A., 1997. Thermodynamic features of the thermal unfolding of human serum albumin. Int. J. Biol. Macromol. 20, 63–73.

Ross, P.D., Finlayson, J.S., Shrake, A., 1984. Thermal stability of human albumin measured by differential scanning calorimetry. II. Effects of isomers of *N*-acetyltryptophanate and tryptophanate, pH, reheating, and dimerization. Vox Sang. 47, 19–27.

Shrake, A., Finlayson, J.S., Ross, P.D., 1984. Thermal stability of human albumin measured by differential scanning calorimetry. I. Effects of caprylate and *N*-acetyltryptophanate. Vox Sang. 47, 7–18.

Storch, H., 1993. Recombinant plasma proteins for therapeutic use—status and developmental trends. Beitr. Infusionsther. 31, 31–37.

Sugii, A., Harada, K., Nishimura, K., Hanaoka, R., Masuda, S., 1989. High performance liquid chromatography of proteins on *N*-methylpyridinium polymer columns. J. Chromatogr. 472, 357–364.

Topczewska-Bruns, J., Pawlak, D., Tankiewicz, A., Chabielska, E., Buczko, W., 2003. Kynurenine metabolism in central nervous system in experimental chronic renal failure. Adv. Exp. Med. Biol. 527, 177–182.

Vogt, W., 1995. Oxidation of methionyl residues in proteins: tools, targets, and reversal. Free Radic. Biol. Med. 18, 93–105.

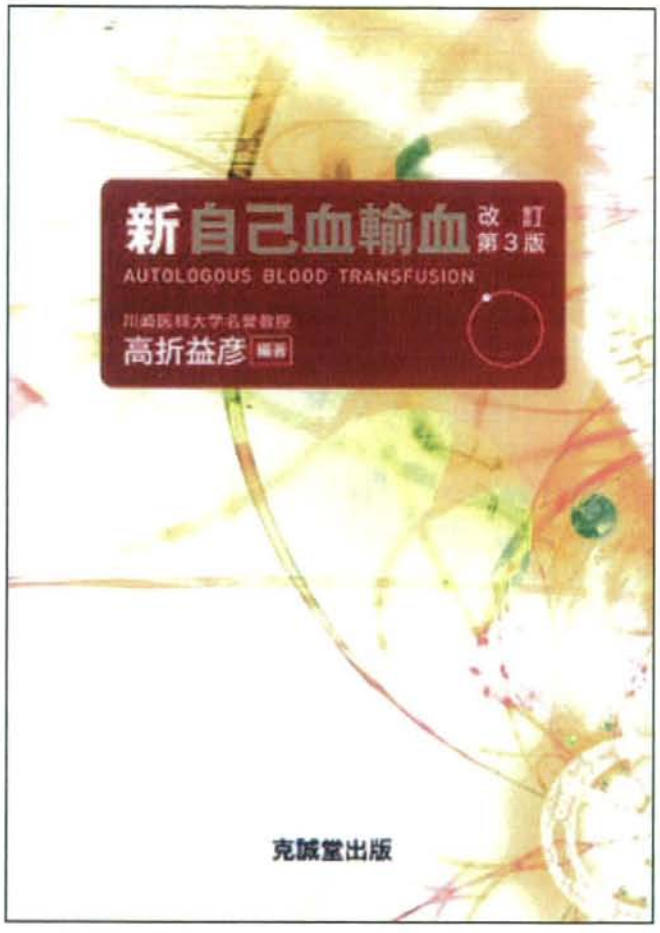
新自己血輸血
改訂第3版
AUTOLOGOUS BLOOD TRANSFUSION
川崎医科大学名誉教授
高折益彦 編著
克誠堂出版

書籍名

新自己血輸血　改訂第3版

出版社

克誠堂出版

著者/特集

高折益彦／編

新自己血輸血　改訂第3版

—目次—

Hemoglobin Vesicles Containing Methemoglobin and L-Tyrosine to Suppress Methemoglobin Formation in Vitro and in Vivo

Tomoyasu Atoji,† Motonari Aihara,† Hiromi Sakai,‡ Eishun Tsuchida,‡ and Shinji Takeoka*,†

Department of Applied Chemistry, Graduate School of Science and Engineering, and Advanced Research Institute for Science and Engineering, Waseda University, Tokyo, 169-8555, Japan. Received December 8, 2005; Revised Manuscript Received July 20, 2006

Hemoglobin (Hb) vesicles have been developed as cellular-type Hb-based O_2 carriers in which a purified and concentrated Hb solution is encapsulated with a phospholipid bilayer membrane. Ferrous Hb molecules within an Hb vesicle were converted to ferric metHb by reacting with reactive oxygen species such as hydrogen peroxide (H_2O_2) generated in the living body or during the autoxidation of oxyHb in the Hb vesicle, and this leads to the loss of O_2 binding ability. The prevention of metHb formation by H_2O_2 in the Hb vesicle is required to prolong the in vivo O_2 carrying ability. We found that a mixed solution of metHb and L-tyrosine (L-Tyr) showed an effective H_2O_2 elimination ability by utilizing the reverse peroxidase activity of metHb with L-Tyr as an electron donor. The time taken for the conversion of half of oxyHb to metHb (T_{50}) was 420 min for the Hb vesicles containing 4 g/dL (620 μM) metHb and 8.5 mM L-Tyr ((metHb/L-Tyr) Hb vesicles), whereas the time of conversion for the conventional Hb vesicles was 25 min by stepwise injection of H_2O_2 (310 μM) in 10 min intervals. Furthermore, in the (metHb/L-Tyr) Hb vesicles, the metHb percentage did not reach 50% even after 48 h under a pO_2 of 40 Torr at 37 °C, whereas T_{50} of the conventional Hb vesicles was 13 h under the same conditions. Moreover, the T_{50} values of the conventional Hb vesicles and the (metHb/L-Tyr) Hb vesicles were 14 and 44 h, respectively, after injection into rats (20 mL/kg), confirming the remarkable inhibitory effect of metHb formation in vivo in the (metHb/L-Tyr) Hb vesicles.

INTRODUCTION

Hemoglobin (Hb)-based O_2 carriers (HBOCs) as red blood cell substitutes have been developed for clinical application in recent years (*1*−*3*). Their safety and usefulness have been demonstrated by many researchers in various fields such as physiology, toxicology, and biochemistry (*4*−*6*). The demand for HBOCs has been increasing year by year due to limitations of donated blood, such as infectious agents, shortage, and storage issues.

HBOCs are generally classified into two types: One is the acellular type, which comprises directly modified Hb molecules such as cross-linked Hb (*7*), polymerized Hb (*8*), and polymer-conjugated Hb (*9*). Some of the acellular-type HBOCs have advanced to phase III clinical trials (*10, 11*). Another kind is the cellular-type Hb systems such as Hb vesicles (*12*) or liposome-encapsulated Hb (*13*), in which Hb molecules are encapsulated with a phospholipid bilayer membrane. Although they are not yet in clinical trials, they have been shown to have excellent O_2 carrying ability and good safety profiles in vivo (*10, 14*−*18*).

Ferrous Hb ($Hb(Fe^{2+})$) molecules of HBOCs gradually lose their O_2 binding ability, because they react with reactive oxygen species (ROS) such as hydrogen peroxide (H_2O_2) (*19, 20*) or nitrogen monoxide (NO*) (*21*) to become nonfunctional ferric Hb ($Hb(Fe^{3+})$, metHb), in addition to the autoxidation of oxyHb molecules themselves. In humans, the concentration of metHb molecules in the red blood cells is usually kept below 1% by reduction systems such as NADH-cytochrome b_5, NADPH-flavin, glutathione, and ascorbic acid. Furthermore, ROS are eliminated by several mechanisms such as superoxide dismutase (SOD), catalase, and peroxidase that help to prevent the metHb formation (*23, 24*). In contrast, metHb generated in the Hb vesicle are not reduced to the ferrous state due to the absence of the reduction systems, because constitutive enzymes and reductants necessary for metHb reduction are removed during the Hb purification process (*25*). The half-life of oxyHb of the Hb vesicles was 14 h in vivo, and more than 90% of oxyHb was converted to metHb within 48 h in the case of 20 vol % top loading to rats (*20*). In human plasma, the concentration of H_2O_2 is reported to be 4−5 μM (*26*) and to elevate to as much as 100−600 μM under inflammatory (*27*) or ischemia-reperfusion conditions (*28*). Therefore, Hb vesicles are required to have an H_2O_2 elimination system for effective prolongation of their O_2 carrying ability. We previously reported that H_2O_2 generated in the living body was the main reason for metHb formation of the Hb vesicles, and the O_2 carrying ability of the Hb vesicles in which catalase was coencapsulated was vastly prolonged in vivo by elimination of H_2O_2 (*20*). Regarding the catalase-coencapsulated vesicles, it is somewhat difficult to obtain a sufficient amount of human catalase from human donated blood. Furthermore, the catalase activity is gradually lost due to denaturation during storage at 25 °C.

Horseradish peroxidase (HRP), which also eliminates H_2O_2 in its enzymatic reaction, is converted to a ferrylHb radical Hb-(Fe^{4+}=O*) state after reaction with H_2O_2, and the radical state is returned to the ferric state by acceptance of two electrons from substrates such as *p*-hydroxyphenylacetic acid (HPA) (*29, 30*). This is a well-known reaction in an H_2O_2 assay method. L-Tyrosine (L-Tyr) dimer or polymer can also be synthesized by an HRP-catalyzed oxidation (*31, 32*). We considered from the above mechanism that if metHb, which has ferric heme like HRP does, could also function as an H_2O_2 elimination enzyme in the presence of L-Tyr as a substrate, then metHb can easily

* Corresponding author. E-mail: takeoka@waseda.jp. Tel: +813-5286-3217. Fax: +813-5286-3217.

† Graduate School of Science and Engineering.

‡ Advanced Research Institute for Science and Engineering.

10.1021/bc050349h CCC: $33.50
Published on Web 09/02/2006

be prepared from purified Hb for the preparation of vesicles. Moreover, L-Tyr itself is an amino acid with high stability and good cost performance. In this study, we prepared Hb vesicles coencapsulating metHb and L-Tyr, thereby incorporating the metHb elimination system into the Hb vesicles themselves. We then evaluated the effect of this coencapsulation on the suppression of metHb formation. Furthermore, we evaluated the safety of the vesicles in vivo.

EXPERIMENTAL PROCEDURES

Purification of Hb from Red Blood Cells (*19, 33*). Hb was purified from outdated human red blood cells provided by the Japanese Red Cross. The red blood cells were washed three times with saline by centrifugation (2000*g*, 10 min) and concentrated by the removal of the supernatant. They were hemolyzed by the addition of an equal volume of water for injection, and then the stroma were removed by ultrafiltration (cutoff M_w 1000 kDa, Biomax-1000V, Millipore Co., Ltd., Bedford). The ligand exchange from O_2 to CO was carried out for the stroma-free Hb solution by CO gas flowing over the stirred solution. The proteins other than HbCO were denatured by heat treatment at 60 °C for 12 h and removed as precipitates. The HbCO solution was fractionated using ultrafiltration filters with a cutoff molecular weight between 1000 kDa and 8 kDa (Biomax-8V, Millipore), followed by concentration with an 8 kDa ultrafilter.

Reaction of Hb Samples with H_2O_2. HbCO was decarbonylated to HbO_2 by the irradiation of visible light to a liquid film of the Hb solution under O_2 atmosphere; potassium ferricyanide was added to the oxyHb solution to convert the oxyHb to metHb (*34*). The conversion of oxyHb to metHb was 99.9% as measured by the modified Evelyn−Malloy method (*35*). After the mixed solution was stirred at 25 °C for 2 h, the potassium ferricyanide was removed from the resulting metHb solution by gel filtration chromatography on Sephadex G-25 (Pharmacia AB, Uppsala). Deferoxamine mesylate (1.6 mM; DFO, Sigma, St. Louis) and L-Tyr (0 or 1 mM; free base, ICN Biomedicals, Inc., Aurora) were added to the oxyHb or metHb solutions, and these solutions were used as Hb samples. Hb samples ([heme] = 20 μM) were reacted with 200 μM H_2O_2 ([heme]/[H_2O_2] = 1/10 molar ratio) in phosphate buffered saline (PBS, pH 7.4 at 37 °C), and the reaction was monitored by the repetitive scanning of a visible region from 300 to 700 nm at 2 min interval by using a UV−vis spectrometer (V-570, Jasco, Tokyo).

For the measurement of H_2O_2 concentrations, samples were reacted with H_2O_2 under the same conditions and were periodically sampled, and the concentration of H_2O_2 was determined spectrofluorometrically by measuring the amount of 6,6′-dihydroxy-[1,1′-biphenyl]-3,3′-diacetic acid (DBDA; Ex. 317 nm; Em. 405 nm), generated by the HRP-catalyzed reaction of HPA with H_2O_2. The final concentrations of HRP and HPA were 4 μM and 6 mM, respectively, and the DBDA concentration was calculated after separating the Hb samples by centrifugal filtration (cutoff 5 kDa, Ultrafree-MC, Millipore, Bedford) (*19, 29*).

Preparation of the Hb Vesicles Containing metHb and L-Tyr ((metHb/L-Tyr) Hb Vesicles) (*36*). MetHb was prepared by the reaction of HbCO (10 g/dL) with an excess amount of potassium ferricyanide. The unreacted potassium ferricyanide and ferrocyanide were removed by ultrafiltration (cutoff M_w 50 kDa, ADVANTEC, Tokyo) until the concentration of potassium ferricyanide was less than 1 μM by monitoring the absorbance with the UV−vis spectrometer. The metHb solution was concentrated to 40 g/dL using a 50 kDa cutoff filter as noted above. HbCO solutions containing 5 or 10 mol % metHb were prepared by mixing the concentrated metHb solution with a 40 g/dL HbCO solution. Pyridoxal 5′-phosphate (PLP, Sigma, St. Louis, MO) was added to the Hb solution as an allosteric effector at a 2.5 equimolar ratio of PLP to HbCO. The L-Tyr solution prepared previously was added to 0.2 N NaOH, and the resulting solution was added to the HbCO/metHb solution. The final concentrations of Hb and L-Tyr in the HbCO/metHb solution were adjusted to 40 g/dL and 1.0 and 8.5 mM, respectively. To prepare the Hb vesicles, powders of 1,2-dipalmitoyl-*sn*-glycero-3-phosphatidylchorine (DPPC), cholesterol, 1,5-bis-*O*-hexadecyl-*N*-succinyl-L-glutaminate (DHSG) (Nippon Fine Chemical Co., Osaka), and 1,2-distearoyl-*sn*-glycero-3-phosphatidylethanolamine-*N*-PEG_{5000} (PEG-DSPE, NOF Co., Tokyo) were mixed at a molar ratio of 5:5:1:0.033 and added to the HbCO/metHb solution, and the mixture was stirred at 25 °C for 12 h. The resulting dispersion of the multilamellar vesicles was subsequently extruded through the nitrocellulose membrane filters with a pore size of 0.22 μm (Fuji Film Co., Tokyo) to prepare the Hb vesicles with an average diameter of 261 ± 30 nm. After the separation of unencapsulated Hb by ultracentrifugation (10000*g*, 60 min), the precipitate of the Hb vesicles was redispersed into saline in order to adjust the Hb concentration of the Hb vesicle dispersion to 10 g/dL. HbCO within the vesicles was decarbonized and oxygenated to HbO_2 by irradiation of visible light onto a liquid film under O_2 atmosphere.

Stepwise Injection of H_2O_2 to a Dispersion of (metHb/L-Tyr) Hb Vesicles. A dispersion of (metHb/L-Tyr) Hb vesicles in PBS (pH 7.4) coencapsulating metHb and L-Tyr (metHb/L-Tyr = 2 g/dL:1 mM, 4 g/dL:1 mM, or 4 g/dL:8.5 mM) was incubated with stirring, and H_2O_2 (310 μM, Ultra Pure Grade, Kanto Chemical Co., Tokyo) was injected in stepwise fashion into the solutions at 10 min intervals. Just before each injection, 20 μL of the dispersion of the (metHb/L-Tyr) Hb vesicles was sampled out, and 20 μL of a catalase solution (50 000 unit) was immediately added for the elimination of the remaining H_2O_2. The percentage of metHb in the (metHb/L-Tyr) Hb vesicles was periodically calculated by the ratio of absorbance at 405 nm (metHb) and 430 nm (deoxyHb) in the Soret band using a UV−vis spectrometer without destruction of the Hb vesicles.

Autoxidation of (metHb/L-Tyr) Hb Vesicles. A dispersion of (metHb/L-Tyr) Hb vesicles was incubated and shaken (120 times/min) under pO_2 of 40 Torr at 37 °C. The percentage of metHb in the vesicles was periodically measured with a UV−vis spectrometer.

Measurement of metHb Formation in the Hb Vesicles in Vivo. Wistar rats (body weight: 240−260 g) were anesthetized with diethyl ether, and a preparation of (metHb/L-Tyr) Hb vesicles containing 4 g/dL of metHb and 8.5 mM of L-Tyr was injected into the tail vein (20 mL/kg, n = 6). Blood was withdrawn from the tail vein and centrifuged (12000*g*, 5 min) to collect the vesicle fraction in the supernatant. The percentage of metHb within the vesicles was measured with a UV−vis spectrometer. The number of blood cells was measured with a blood cell counter (Sysmex, KX-21, Kobe).

RESULTS AND DISCUSSION

Reaction of the L-Tyr Containing metHb Solution with H_2O_2. We added H_2O_2 to the metHb solution (5 μM) with or without 1 mM L-Tyr. Figure 1 shows the changes of the H_2O_2 concentration in the metHb solutions with and without L-Tyr. The initial elimination rates of H_2O_2 in the metHb solutions were calculated on the basis of a pseudo-first-order rate law. The elimination rates with and without L-Tyr at 37 °C were 3.0×10^3 and 3.2×10^4 M^{-1} s^{-1}, respectively. The apparent rate constant of the metHb solution containing L-Tyr was about 10 times larger than that with the metHb solution alone, and this

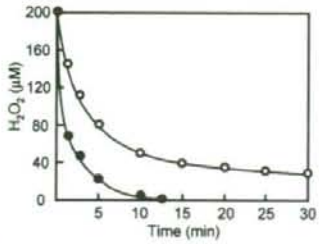

Figure 1. Time course of H_2O_2 elimination by (○) metHb (5 μM) (●) metHb (5 μM) + L-Tyr (1 mM) during the reaction with 200 μM of H_2O_2 at 37 °C.

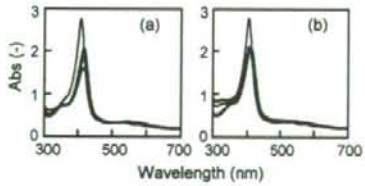

Figure 2. UV−vis spectral changes of (a) a metHb (5 μM) solution and (b) a metHb (5 μM) solution containing L-Tyr (1 mM) during the reaction with 200 μM H_2O_2 ([heme]:[H_2O_2] = = 1/10) at 37 °C. The scanning was performed at 4 min intervals, immediately after the addition of H_2O_2 solution to each Hb solution.

value was estimated to be approximately equal to the 150 units of catalase. Moreover, around 40 μM H_2O_2 remained after a 30 min reaction of 200 μM H_2O_2 in the metHb solution alone, whereas H_2O_2 was completely eliminated within 15 min in the metHb solution containing L-Tyr.

The UV−vis spectral changes during the reaction of H_2O_2 in the metHb solution (5 μM) and the metHb solution containing L-Tyr (1 mM) are shown in Figure 2a and b, respectively. In the case of metHb alone, there was a shift in the spectrum of metHb, namely, the Soret band of metHb (405 nm) was shifted to 417 nm, and the typical metHb peak at 630 nm was completely abolished, which indicated a change to a different form of metHb. There was a time-dependent decrease in peak intensities, indicating the degradation of this intermediate form of Hb during the reaction of H_2O_2. We speculated that this intermediate form of Hb was ferrylHb radical. It has been reported that the ferrylHb radical is formed by the reaction of metHb with H_2O_2 (*37*). Furthermore, the stoichiometry of metHb (5 μM) and the reacted H_2O_2 (200 μM) suggests that the metHb worked as an enzyme such as catalase, although the stability of the enzyme was low and it was degraded. Because the Fenton reaction can be prevented by the addition of DFO, which is a chelator of Fe^{3+}, this enzymatic H_2O_2 elimination was considered to be a pseudo-catalase-like reaction of metHb. Conversely, the metHb solution with L-Tyr showed a fast spectral change and then stayed constant during the reaction, as shown in Figure 2b. Also, the small spectral shift of the metHb solution with L-Tyr suggested that the metHb reacted with H_2O_2 was converted to the ferrylHb radical. The ratio of metHb to ferrylHb should be constant during reaction with H_2O_2. Comparing with the reaction mechanism of peroxidase, where the ferric state is converted to the ferrylHb radical state by the reaction of H_2O_2 to produce H_2O, and then the ferryl radical state is recovered to the ferric state by one-electron oxidation of two substrate molecules to generate another molecule of H_2O, we could compare, in this case, the peroxidase and the substrate to metHb and L-Tyr, respectively. More precisely, we could describe the enzymatic reaction as reverse peroxidation, and the substrate as H_2O_2 where L-Tyr works as an electron donor. Furthermore, we detected L-Tyr dimer (L-Tyr-L-Tyr (diTyr)), which was

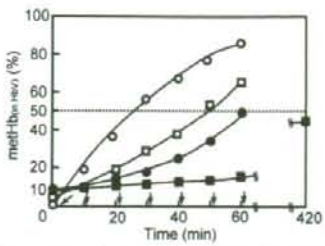

Figure 3. Time course of metHb formation in Hb vesicles at 37 °C during the stepwise addition of H_2O_2 (310 μM) to 5 g/dL Hb vesicle dispersions coencapsulating (●) 4 g/dL metHb and 1 mM L-Tyr, (□) 2 g/dL metHb and 1 mM L-Tyr, (■) 4 g/dL metHb and 8.5 mM L-Tyr, and (○) no metHb and L-Tyr.

produced from the coupling of the two L-Tyr radicals in their ortho position. Such a stable reaction of the unstable ferrylHb radical to metHb by L-Tyr would help the stable elimination reaction of H_2O_2. Therefore, we aimed to construct this system in the Hb vesicles.

H_2O_2 Stepwise Addition to the (metHb/L-Tyr) Hb Vesicles. Figure 3 shows the time course of metHb formation in the conventional Hb vesicles or the (metHb/L-Tyr) Hb vesicles by stepwise injection of H_2O_2 (310 μM) in 10 min intervals. H_2O_2 (310 M) injection to a 5 g/dL conventional Hb vesicle dispersion ([heme] = 3.1 mM) showed an elevation in the metHb percentage with increasing injections of H_2O_2, and the percentage of metHb reached 85% after 60 min (6 injections). However, the (metHb/L-Tyr) Hb vesicles (metHb/L-Tyr = 2 g/dL:1 mM, 4 g/dL:1 mM) showed a significant suppression of metHb formation in the vesicles. The metHb percentages of these Hb vesicles were 67% and 50% after 60 min (6 injections), respectively. Furthermore, by increasing the amount of L-Tyr to 8.5 mM (metHb: 4 g/dL), metHb formation was dramatically suppressed; the percentages were 17% and 45% after 60 and 420 min, respectively (6 and 42 injections, respectively).

From these results, it was confirmed that the formation of metHb from oxyHb by reaction with H_2O_2 was suppressed by the H_2O_2 elimination system of metHb and L-Tyr. Moreover, the persistence of the metHb suppression effect depends on the amount of metHb as an enzyme and L-Tyr as a substrate. The solubility of L-Tyr in pure water is 1.2 mM; however, we succeeded in preparation of an Hb solution containing 8.5 mM L-Tyr by using an alkali solution (NaOH) and the interaction of L-Tyr with highly concentrated Hb molecule (40 g/dL). We succeeded in the construction of Hb vesicles having an H_2O_2 elimination system using Hb only as protein or enzyme.

Autoxidation of the (metHb/L-Tyr) Hb Vesicles. Besides the formation of metHb by H_2O_2, oxyHb is automatically oxidized to metHb, initiated by one-electron reduction of a coordinated dioxygen molecule to generate superoxide anion radical ($O_2^{-\bullet}$). MetHb formation in vesicles by such autoxidation was measured under the condition of the pO_2 of 40 Torr at 37 °C, because at this pO_2 value, the rate of metHb formation is maximal (*38*). In the conventional Hb vesicles, the percentage of metHb periodically increased by autoxidation of oxyHb in the vesicles. The T_{50} was 13 h, and the metHb percentage reached 90% after 24 h incubation (Figure 4). On the other hand, the metHb formation of the Hb vesicles containing 4 g/dL metHb and 1 mM L-Tyr was effectively suppressed; the T_{50} was 24 h. Furthermore, in the Hb vesicles containing 4 g/dL metHb and 8.5 mM L-Tyr, the percentage of metHb formed was 20% and 43% after 24 and 48 h, respectively, and did not reach 50% when the measurement ended (48 h).

Autoxidation of oxyHb is also an important factor of metHb formation. The autoxidation rate of oxyHb depends on many factors such as the O_2 affinity, P_{50}, the pO_2, temperature, and

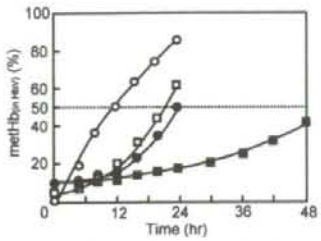

Figure 4. Time course of metHb formation in Hb vesicles under pO_2 of 40 Torr at 37 °C during autoxidation of 5 g/dL Hb vesicle dispersion coencapsulating (●) 4 g/dL metHb and 1 mM L-Tyr, (□) 2 g/dL metHb and 1 mM L-Tyr, (■) 4 g/dL metHb and 8.5 mM L-Tyr, and (○) no metHb and L-Tyr.

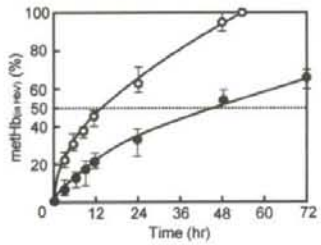

Figure 5. Time course of metHb formation in Hb vesicles injected into Wistar rats (20 mL/kg). Hb vesicles were encapsulating (●) 4 g/dL metHb and 8.5 mM L-Tyr, and (○) no metHb and L-Tyr.

pH. OxyHb molecules in the Hb vesicles are also influenced by these same factors, though the rates could be different from that of the oxyHb solution. The half-life of oxyHb to metHb (T_{50}) in the conventional Hb vesicles (P_{50} = 33 Torr) at 37 °C was about 12 h, shorter than that of the oxyHb solution (T_{50} = 24 h, PBS, pH 7.4). The autoxidation rate of the Hb vesicles containing metHb and L-Tyr was also effectively reduced in a similar way to that observed in the above experiment of H_2O_2 stepwise addition. The reason could be that the autoxidation of oxyHb is additionally influenced by H_2O_2. A superoxide anion radical (O_2^{-}*) generated by the oxyHb autoxidation is spontaneously converted to H_2O_2 in the presence of H^+. This H_2O_2 attacks the other oxyHb molecules. Therefore, the elimination of the H_2O_2 would result in the suppression of the autoxidation rate of oxyHb in the Hb vesicles.

Measurement of metHb Formation in (metHb/L-Tyr) Hb Vesicles in Vivo. Figure 5 shows the percentage of generated metHb after the intravenous injection (20 mL/kg) of the conventional Hb vesicles or the (metHb/L-Tyr) Hb vesicles into the tail vein of Wistar rats (n = 6). The metHb percentages of the conventional Hb vesicles and the (metHb/L-Tyr) Hb vesicles after 4 h were 22% and 18%, respectively, and the T_{50} values were 14 and 44 h, respectively. Furthermore, the Wistar rats were all alive for 72 h after the measurement, at which time they were sacrificed, indicating the safety of this system in vivo. These results confirmed the suppressive effect of metHb formation in vivo using the (metHb/L-Tyr) Hb vesicles.

In a previous study, we coencapsulated catalase to eliminate H_2O_2 generated in vivo, thus suppressing the formation of metHb within Hb vesicles, and we confirmed the suppression of metHb formation (*20*). The T_{50} of the catalase-coencapsulated Hb vesicles was 37 h with a catalase concentration of 4.2 × 10^4 unit/mL (0.5 g/dL catalase as a protein concentration). We estimated that the concentration of catalase was the amount at the saturation point of T_{50} prolongation, because the same T_{50} was obtained when 5.6 × 10^4 unit/mL catalase was used for coencapsulation. In comparison with these results, the (metHb/L-Tyr) system was more effective in the suppression of metHb formation by elimination of H_2O_2. It is thought that catalase activity is gradually lost at 37 °C in vivo (*20*), whereas the activity of the (metHb/L-Tyr) system should be very stable at 37 °C, and the amount of L-Tyr (8.5 mM within the Hb vesicle) was sufficient to eliminate H_2O_2 in the Hb vesicles. From these results, the increase of the metHb percentage of the (metHb/L-Tyr) Hb vesicles is likely due to the autoxidation of Hb, which is impossible to suppress in this system.

ACKNOWLEDGMENT

The authors thank Dr. K. Ohta at Oxygenix Co., Ltd., for technical advice about in vivo measurement of (metHb/L-Tyr) Hb vesicles. This work was supported in part by Health and Labor Science Research Grant, Ministry of Health, Labor and Welfare, Japan, Grant-in-Scientific Research (18500368), and 21COE "Practical Nano-Chemistry" and "Consolidated Research Institute for Advanced Science and Medical Care" from MEXT, Japan.

LITERATURE CITED

(1) Tsuchida, E. (1995) *Artificial Red Cells*, John Wiley and Sons, New York.
(2) Winslow, R. M. (1997) Progress on blood substitutes. *Nat. Med. 3*, 474−474.
(3) Chang, T. M. S. (1997) *Blood Substitutes: Principles, Methods, Products and Clinical Trials*, S. Karger AG, Switzerland.
(4) Tsuchida, E., Ed. (1998) *Blood Substitutes: present and future perspectives*, Elsevier Science, Amsterdam.
(5) Reiss, J. G. (2001) Oxygen carriers ("blood substitutes")-raison d'etre, chemistry, and some physiology. *Chem. Rev. 101*, 2797−2920.
(6) D'Agnillo, F., and Alayash, A. I. (2001) Redox cycling of diaspirin cross-liked hemoglobin induced G2/M arrest and apoptosis in cultured endothelial cells. *Blood 98*, 3315−3323.
(7) Przybelski, R. J., Dairy, E. K., and Birnbaum, M. L. (1997) The pressor of effect of hemoglobin − good or bad? In *Advances in Blood Substitutes: Industrial Opportunities and Medical Challenges* (Winslow, R. M., Vandegriff, K. D., and Intaglietta, M., Eds.) Birkhauser, Boston.
(8) Gould, S. A., Moore, E. E., Hoyt, D. B., Burch, J. M., Haenel, J. B., Garcia, J., DeWoskin, R., and Moss, G. S. (1998) The first randomized trial of human polymerized hemoglobin as a blood substitute in acute trauma and emergency surgery. *J. Am. Coll. Surg. 187*, 113−122.
(9) McCarthy, M. R., Vandegriff, K. D., and Winslow, R. M. (2001) The role of facilitated diffusion in oxygen transport by cell-free hemoglobins: implications for the design of hemoglobin-based oxygen carriers. *Biophys. Chem. 92*, 103−117.
(10) Mullon, J., Giacoppe, G., Clagett, C., McCune, D., and Dillard, T. (2000) Transfusions of polymerized bovine hemoglobin in a patient with severe sutoimmune hemolytic anemia. *N. Engl. J. Med. 342*, 1638−1643.
(11) Sloan, E. P., Koenigsberg, M., Gens, D., Cipolle, M., Runge, J., Mallory, M. N., and Rodman, G., Jr. (1999) Diaspirin cross-linked hemoglobin (DCLHb) in the treatment of severe traumatic hemorrhagic shock: a randomized controlled efficacy. *JAMA 282*, 1857−1864.
(12) Sakai, H., Horinouchi, H., Tomiyama, K., Ikeda, E., Takeoka, S., Kobayashi, K., and Tsuchida, E. (2001) Hemoglobin-vesicles as oxygen carriers. Influence on phagocytic activity and histopathological changes in reticuloendothelial system. *Am. J. Pathol. 159*, 1079−1088.
(13) Rudolph, A. S., Sulpizio, A., Hieble, P., MacDonald, V., Chavez, M., and Feuerstein, G. (1997) Liposome encapsulating attenuates hemoglobin-induced vasoconstriction inrabbit arterial segment. *J. Appl. Physiol. 82*, 1826−1835.
(14) Sakai, H., Cabrales, P., Tsai, A. G., Tsuchida, E., and Intaglietta, M. (2005) Oxygen release from low and normal P_{50} Hb vesicles in transiently occluded arterioles of the hamster window model. *Am. J. Physiol. 288*, H2897−H2903.

(15) Cabrales, P., Sakai, H., Tsai, A. G., Takeoka, S., Tsuchida, E., and Intaglietta, M. (2005) Oxygen transport by low and normal oxygen affinity hemoglobin vesicles in extreme hemodilution. *Am. J. Physiol. 288*, H1885−H1892.

(16) Sakai, H., Masada, Y., Horinouchi, H., Ikeda, E., Sou, K., Takeoka, S., Suematsu, M., Takaori, M., Kobayashi, K., and Tsuchida, E. (2004) Physiological capacity of the reticuloendothelial system for the degradation of hemoglobin vesicles (artificial oxygen carriers) after massive intravenous doses by daily repeated infusions for 14 days. *J. Pharmacol. Exp. Ther. 311*, 874−884.

(17) Yoshizu, A., Izumi, Y., Park, S., Sakai, H., Takeoka, S., Horinouchi, H., Ikeda, E., Tsuchida, E., and Kobayashi, K. (2004) Hemorrhagic shock resuscitation with an artificial oxygen carrier, hemoglobin vesicle, maintains intestinal perfusion and suppresses the increase in plasma tumor necrosis factor-α. *ASAIO J. 50*, 458−463.

(18) Sakai, H., Takeoka, S., Park, S. I., Kose, T., Hamada, K., Izumi, Y., Yoshizu, A., Nishide, H., Kobayashi, K., and Tsuchida, E. (1997) Surface modification of hemoglobin vesicles with poly(ethylene glycol) and effects on aggregation, viscosity, and blood flow during 90% exchange transfusion in anesthetized rats. *Bioconjugate Chem. 8*, 23−30.

(19) Takeoka, S., Teramura, Y., Atoji, T., and Tsuchida, E. (2002) Effect of Hb-encapsulation with vesicles on H_2O_2 reaction and lipid peroxidation. *Bioconjugate Chem. 13*, 1302−1308.

(20) Teramura, Y., Kanazawa, H., Sakai, H., Takeoka, S., and Tsuchida, E. (2003) Prolonged oxygen-carrying ability of hemoglobin vesicles by coencapsulation of catalase in vivo. *Bioconjugate Chem. 14*, 1171−1176.

(21) Herold, S., and Rock, G. (2003) Reactions of deoxy-, oxy-, and methemoglobin with nitrogen monoxide. *J. Biol. Chem. 278*, 6623−6634.

(22) Shikama, K. (1998) The molecular mechanism of autoxidation for myoglobin and hemoglobin: A venerable puzzle. *Chem. Rev. 98*, 1357−1373.

(23) Shikama, K. (1984) A controversy on the mechanism of autoxidation of oxymyoglobin and oxyhemoglobin: oxidation, dissociation, or displacement? *Biochem. J. 223*, 279−280.

(24) Tomoda, A., Yoneyama, T., and Tsuji, A. (1981) Changes in intermediate hemoglobins during autoxidation of hemoglobin. *Biochem. J. 195*, 485−492.

(25) Naito, Y., Fukutomi, I., Masada, Y., Sakai, H., Takeoka, S., Tsuchida, E., Abe, H., Hirayama, J., Ikebuchi, K., and Ikeda, H. (2002) Virus removal from hemoglobin solution using Planova membrane. *J. Artif. Organs 5*, 141−145.

(26) Nagababu, E., and Rifkind, J. M. (2000) Reaction of hydrogen peroxide with ferrylhemoglobin: superoxide production and heme degradation. *Biochemistry 39*, 12503−12511.

(27) Gunther, M. R., Sampath, V., and Caughey, W. S. (1999) Potential roles of myoglobin autoxidation in myocardial ischemia-reperfusion injury. *Free Radical Biol. Med. 26*, 1388−1395.

(28) Svistunenko, D. A., Patel, R. P., Voloshchenko, S. V., and Wilson, M. T. (1997) The globin-based free radical of ferryl hemoglobin is detected in normal human blood. *J. Biol. Chem. 272*, 7114−7121.

(29) Hofmann, F., Hofmann, L., Hubl, W., and Meissner, D. (1984) Determination of horseradish peroxidase (HRP) with the substrates H_2O_2 and *p*-hydroxyphenylacetic acid (HPA) in the fluorescence enzyme immunoassay. *Z. Med. Laboratoriumsdiagn. 25*, 14−21.

(30) Yusa, K., and Shikama, K. (1987) Oxidation of oxymyoglobin to metmyoglobin with hydrogen peroxide: involvement of ferryl intermediate. *Biochemistry 26*, 6684−6688.

(31) Fukuoka, T., Tachibana, Y., Tonami, H., Uyama, H., and Kobayashi, S. (2002) Enzymatic polymerization of tyrosine derivatives. peroxidase- and protease-catalyzed synthesis of poly(tyrosine)s with different structures. *Biomacromolecules 3*, 768−774.

(32) Malencik, D. A., Sprouse, J. F., Swanson, C. A., and Anderson, S. R. (1996) Dityrosine: preparation, isolation, and analysis. *Anal. Biochem. 242*, 202−213.

(33) Hinsberg, W. D., Milby, K. H., and Zare, R. N. (1981) Determination of insulin in serum by enzyme immunoassay with fluorimetric detection. *Anal. Chem. 53*, 1509−1512.

(34) Sakai, H., Onuma, H., Umeyama, M., Takeoka, S., and Tsuchida, E. (2000) Photoreduction of methemoglobin by irradiation in the near-ultraviolet region. *Biochemistry 39*, 14595−14602.

(35) Van Assendelft, O. W. (1970) *Spectrophotometer of hemoglobin derivatives*, Royal Vangorcum Ltd., Assen, The Netherlands.

(36) Sakai, H., Hamada, K., Takaoka, S., Nishide, H., and Tsuchida, E. (1996) Physical properties of hemoglobin vesicles as red cell substitutes. *Biotechnol. Prog. 12*, 119−125.

(37) Cashon, R. E., and Alayash, A. I. (1995) Reaction of human hemoglobin HbA_0 and two cross-linked derivatives with hydrogen peroxide: differential behavior of the ferryl intermediate. *Arch. Biochem. Biophys. 316*, 461−469.

(38) Takeoka, S., Sakai, H., Kose, T., Mano, Y., Seino, Y., Nishide, H., and Tsuchida, E. (1997) Methemoglobin formation in hemoglobin vesicles and reduction by encapsulated thiols. *Bioconjugate Chem. 8*, 539−544.

BC050349H

Biomedical Research 27 (6) 283-288, 2006

Fluid resuscitation with hemoglobin-vesicle solution does not increase hypoxia or inflammatory responses in moderate hemorrhagic shock

Yoshitugu GOTO[1], Katsuyuki TERAJIMA[1], Takaya TSUESHITA[1], Masao MIYASHITA[2], Hirohisa HORINOUCHI[3], Hiromi SAKAI[4], Eishun TSUCHIDA[4] and Atsuhiro SAKAMOTO[1]

[1] Department of Anesthesiology and [2] Department of Surgery, Nippon Medical School; [3] Department of Surgery, School of Medicine, Keio University; and [4] Advanced Research Institute for Science and Engineering, Waseda University

(Received 22 September 2006; and accepted 26 October 2006)

ABSTRACT

The aim of the present study was to compare the hypoxic and inflammatory effects of transfusing hemoglobin-vesicles (HbV) or lactated Ringer's (LR) solution on several organs in a hemorrhagic shock model. Hemorrhagic shock was induced in 48 anesthetized rats by withdrawing 28 mL/kg blood. The animals were resuscitated by replacing the blood with an equal volume of HbV solution or three times the volume of LR solution. The heart, lung, liver, kidney and spleen were extracted at different time points following resuscitation, and mRNA expression levels of hypoxia-induced factor 1-alpha (HIF-1α) and tumor necrosis factor-alpha (TNF-α) were determined. Blood lactate concentrations in the HbV group rapidly returned to baseline levels, whereas elevated lactate concentrations in the LR group were prolonged. There were no significant differences between the two resuscitation groups in terms of HIF-1α and TNF-α expression in the organs examined. HIF-1α and TNF-α expression in the lungs was significantly greater than in other organs. Our results suggest that resuscitation from hemorrhagic shock with HbV did not increase hypoxic or inflammatory effects in major organs, compared with resuscitation using LR solution, despite prolonged elevation of blood lactate.

Hemorrhagic shock is caused by hypovolemia and a loss of blood components, and it is usually corrected by infusion of crystalloids and colloids. Decreased blood flow and/or reduction in hemoglobin (Hb) during hemorrhagic shock can, however, lead to tissue hypoxia and critical anemia, which requires red blood cell (RBC) transfusion. During emergency care or perioperative periods in which RBCs are not available, RBC substitutes, such as those derived from Hb, are used (5, 8, 18, 28).

Hb-based oxygen carriers (HBOCs) are a valuable resource in prehospital care, large-scale disasters, and remote hospitals, in which stored blood is either not available or is rapidly depleted. The safety and efficacy of HBOCs can be evaluated in terms of hemodynamics (28), systemic and regional vasoconstriction (10, 11), tissue oxygenation, immunomodulation (13), and post-injury multiple organ failure (MOF) (20).

The standard approach to restoring oxygen delivery in hemorrhagic shock has been crystalloid administration to expand intravascular volume, followed by stored RBCs for critical anemia. However, the initial transfusion therapy after hemorrhagic shock may have adverse immunoinflammatory effects that increase the risk of MOF (20, 27, 32). Hb vesicles (HbV) are artificial oxygen carriers (24, 25, 28, 31). They consist of phospholipid vesicles (liposomes) that encapsulate purified human Hb with polyethylene glycol chains at the surface. The aim

Address correspondence to: Dr. Katsuyuki Terajima
Department of Anesthesiology, Nippon Medical School, 1-1-5, Sendagi, Bunkyo-ku, Tokyo, 113-8603, Japan
Tel: +81-3-3822-2131 ext. 6748, Fax: +81-3-5685-3077
E-mail: terajima.katsuyuki@nifty.com

of the present study was to evaluate the use of HbV during resuscitation following hemorrhagic shock and to determine its oxygenation and proinflammation effects on multiple organs.

MATERIALS AND METHODS

Animal preparation. This study was approved by the Ethics Committee for Animal Experiments at Nippon Medical School, Japan. A total of 48 male Sprague-Dawley rats, aged 10 to 13 weeks weighing 308 ± 43 g (mean ± standard deviation (SD)), were anesthetized with 2–4% sevoflurane. Heated blankets were used to maintain core body temperature at 37°C. Lactated Ringer's solution (LR) was infused at a rate of 1 mL/kg/h via the tail vein, until baseline blood pressure measurements were obtained.

Following laparotomy, a 24G Teflon catheter was inserted into the inferior vena cava, and the common iliac artery was catheterized to allow mean arterial blood pressure (MAP) measurement and blood withdrawal for inducing hemorrhagic shock. Arterial pressure and central venous pressure (CVP) were measured with a pressure transducer (TP-300T; Nihon Koden, Tokyo, Japan) for 2 h following fluid resuscitation. The transducer was connected to a computer and electronic signals were configured to represent pressure changes by analysis software (MacLab/s; ADInstruments Japan, Nagoya, Japan).

Experimental procedure. Fifteen minutes after the preparation was complete, hemorrhagic shock was induced by withdrawing 28 mL/kg blood over 20 min, and maintaining the state for 15 min without fluid resuscitation. Animals were then randomly assigned to one of eight groups (n = 6 per group) based on treatment and time of sacrifice. Animals were resuscitated by infusing HbV solution (Oxygenix Co. Ltd., Tokyo, Japan, [Hb] = 10 g/dL) at the same volume as LR or by infusing three times the volume of LR. Each group was described according to the method of fluid resuscitation and the time of intentional sacrifice from the fluid resuscitation (*e.g.*, the group, which includes the animals resuscitated using HbV solution and sacrificed 2 h after the resuscitation, was described as HbV-2H). Arterial blood (0.2 mL) was sampled before hemorrhagic shock (baseline), after hemorrhagic shock (T1), and 1 h (T2) and 2 h (T3) after fluid resuscitation. An ABL 700 (Radiometer A/S, Copenhagen, Denmark) was used to measure Hb concentration, hematocrit, blood lactate concentration and pO2. MAP and CVP were recorded before and after blood withdrawal and 1 h and 2 h after fluid resuscitation.

RNA extraction and RT-PCR. Following a 2 h observation period, the heart, lung, liver, kidney, and spleen of animals in the 3XLR-2H and HbV-2H groups were removed. The same organs were removed from the remaining rats 24, 72, and 168 h after resuscitation under sevoflurane anesthesia. Organs were placed in liquid nitrogen and stored at −80°C pending RNA extraction. RNA isolation, quantification, and RT-PCR were performed according to established methods (6, 26).

Briefly, total RNA was extracted from each tissue sample using the chaotrophic Trizol method followed by Isogen-chloroform extraction and isopropanol precipitation. Residual genomic DNA was eliminated with DNase I (Takara Shuzo, Otsu, Japan). One microgram of each total RNA sample was reverse transcribed at 37°C for 1 h in a 20 μL solution with mouse Moloney leukemia virus reverse transcriptase and hexanucleotide random primers (Takara Shuzo). RNA was quantified by measuring absorbance at 260 nm, and each sample was diluted to 0.4 μg/μL.

PCR primers and TaqMan fluorogenic probes were designed using the Primer Express software program (Applied Biosystems, Foster City, CA) and had the following sequences: Glyceraldehyde 3-phosphate dehydrogenase (GAPDH): forward 5'-GAAGGTGAAGGTCGGAGTC-3', reverse 5'-GAAGATGGTGATGGGATTTC-3', and probe FAM-CAAGCTTCCCGTTCTCAGCC-Tamra. TNF-α: forward 5'-GCCTCAGCCTCTTCTCATTCCT-3', reverse 5'-GATGAGAGGGAGCCCATTTG-3', and probe FAM-ACCACGCTCTTCTGTCT-Tamra. HIF-1α: forward 5'-CACCTTCTACCCAAGTACCTCAAGA-3', reverse 5'-TGTCCGACTGTGAGTACCACTGT-3', probe FAM-ACCACTGCTAAGGCAT-Tamra. GAPDH was used as the housekeeping gene.

Quantitative PCR was carried out in a 50 μL solution containing 20 ng cDNA, 25 μL TaqMan Universal Master Mix (Applied Biosystems, Foster City, CA), 900 nM forward and reverse primers, 200 nM TaqMan probe and deionized water. PCR conditions were 50°C for 2 min and 95°C for 10 min followed by 40 cycles of 95°C for 15 s and 60°C for 1 min. The 6-FAM-labeled TaqMan probe was cleaved during amplification to generate a fluorescent signal that was measured using an ABI PRISM 5700 Sequence Detector (Applied Biosystems). Samples and calibration curve samples were run in triplicate. Values were interpolated automatically from the standard curve. A similar system utilizing a separate

GAPDH probe and primer set (TaqMan GAPDH control reagent kit; Applied Biosystems) was designed and run for GAPDH along with each sample to correct for total nucleic acid content. Relative amounts of mRNA were calculated by the comparative critical threshold (CT) method (Applied Biosystems).

Statistical analysis. Data are expressed as mean ± SD. Statistical analyses were performed with Statview® version 5.0 for Macintosh software (Abacus Concepts Inc., Berkley, CA). Differences in MAP, CVP, Hb concentration, blood lactate concentration and gene expression between resuscitation groups and time after resuscitation were analyzed with two-factor factorial ANOVA and the Tukey-Kramer test at the 95% confidence level. Within group differences were analyzed with one-factor ANOVA and the Tukey-Kramer test for comparison with each baseline value. p-values < 0.05 were considered statistically significant.

RESULTS

All rats tolerated hemorrhagic shock, and received fluid resuscitation period and survived until the time of sacrifice. MAP and CVP at baseline were similar in the 3XLR and HbV groups (Table 1). MAP was significantly reduced by hemorrhagic shock and returned to baseline values by fluid resuscitation in both groups. Hemorrhagic shock reduced CVP and fluid resuscitation increased CVP, but not significant. MAP was decreased in 3XLR group 2 h after resuscitation. Arterial blood lactate concentrations at baseline did not differ significantly between the 3XLR and HbV groups. Hemorrhagic shock increased arterial blood lactate concentration. Fluid resuscitation using HbV solution reduced the lactate level, but lactate concentrations in the 3XLR group remained elevated compared to baseline. Hb concentration and hematocrit at baseline were similar in both groups. After the fluid resuscitation, the Hb concentration and hematocrit in the HbV group were significantly higher than in the 3XLR group.

Expression of HIF-1α and TNF-α mRNA at various time points after fluid resuscitation is shown in Figs. 1 and 2. There were no significant differences in gene expression in any organ between the 3XLR and HbV groups. However, HIF-1α expression in the lung was significantly higher than in the heart, liver, and kidney in both 3XLR and HbV groups (Fig. 1). HIF-1α mRNA expressions in the heart were significantly lower than in the lung and spleen. HIF-1α mRNA expression peaked 24 h after fluid resuscitation and then decreased in the most organs. In contrast, TNF-α mRNA gradually increased during the 168 h following resuscitation (Fig. 2). TNF-α expression in the lung was significantly higher than in the other organs examined.

Table 1 *Hemodynamics and arterial blood values*

Measurement	Time point			
	Baseline	T1	T2	T3
Mean arterial blood pressure (mmHg)				
3XLR	83.3 ± 9.2	32.5 ± 4.0†	80.0 ± 13.7	56.0 ± 20.4†
HbV	80.5 ± 13.7	30.2 ± 3.1†	87.8 ± 14.8	68.7 ± 5.3
Central venous pressure (mmHg)				
3XLR	4.0 ± 0.6	3.3 ± 1.9	4.5 ± 1.4	3.7 ± 0.5
HbV	4.2 ± 1.2	4.0 ± 0.9	5.2 ± 2.1	4.7 ± 2.0
Hemoglobin concentration (g/dL)				
3XLR	11.1 ± 2.2	8.5 ± 2.4	7.4 ± 0.7†	8.0 ± 1.3†
HbV*	13.2 ± 1.5	9.5 ± 3.0†	13.5 ± 0.6	13.0 ± 2.1
Hematocrit (%)				
3XLR	34.2 ± 6.7	26.4 ± 7.1	23.0 ± 2.2†	24.9 ± 3.7†
HbV*	40.4 ± 4.6	29.4 ± 9.0†	41.6 ± 2.0	40.1 ± 6.3
Blood Lactate concentration (mmol/L)				
3XLR	2.1 ± 0.9	6.7 ± 2.6†	6.3 ± 2.6†	4.6 ± 2.7
HbV	3.2 ± 1.1	5.8 ± 1.0†	2.6 ± 0.5	2.6 ± 0.3

T1, immediately after fluid resuscitation; T2, 1 h after resuscitation; T3, 2 h after resuscitation

† significantly different than baseline ($p < 0.05$)

*significantly different than LR group ($p < 0.05$)

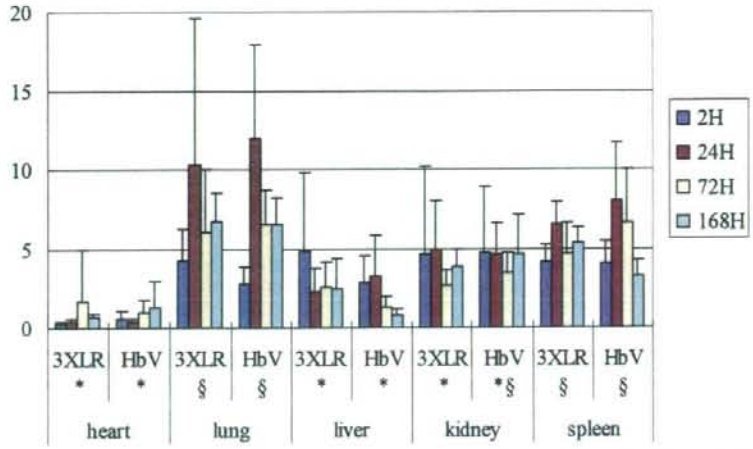

Fig. 1 HIF-1 α mRNA expression. *significantly different from lung ($p < 0.05$), § significantly different from heart ($p < 0.05$)

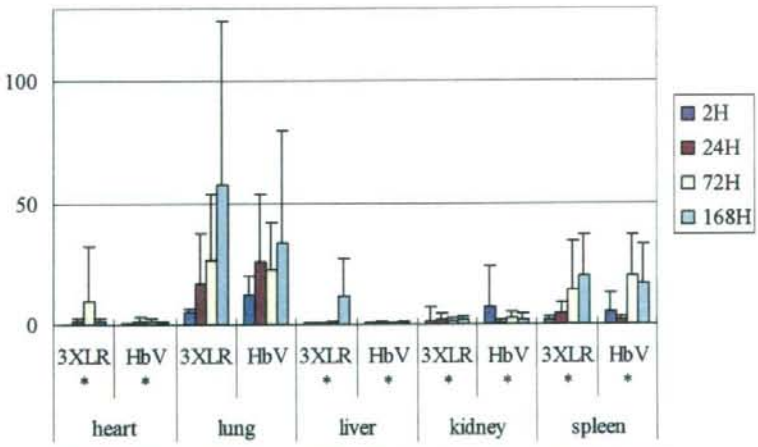

Fig. 2 TNF-α mRNA expression. *significantly different from lung ($p < 0.05$)

DISCUSSION

Critical acute anemia during emergency care and the perioperative period is usually treated with RBC transfusion. However, this requires time-consuming blood typing and cross matching tests, and the preservation time of blood products is limited. Stored RBCs cannot be supplied during prehospital care, and costs are incurred for their transport to remote hospitals. Moreover, there is increasing evidence that RBC transfusions are associated with adverse effects on the immune response to injury and illness (27). Transfusion of more than six units of RBCs within the first 12 h after injury is an independent risk factor for MOF (20), and aged packed RBC transfusion further increases the risk of postinjury MOF (32). HBOCs may attenuate adverse immunoinflammatory effects induced by allogenic RBC transfusion and ultimately reduce the incidence of postinjury acute respiratory distress syndrome (ARDS) and MOF (19).

In the present study, organ hypoxia and proinflammatory reactions were revealed by measuring HIF-1α and TNF-α mRNA expression after fluid resuscitation with crystalloid LR or HbV solutions. Despite a rapid recovery from elevated blood lactate

concentrations in the HbV group, no significant group differences were found in the expression of HIF-1α or TNF-α in intrathoracic and splanchnic organs. A reduction in hemorrhagic volume is sufficient to depress MAP and increase blood lactate concentrations, leading to a 40–50% loss of circulating volume (24, 25, 31). Infection and bacterial translocation in the gut, which commonly occur after injury, and coincidental hemorrhagic shock, can also prolong the increased HIF-1α response (14). Although fluid resuscitation for hemorrhagic shock using HbV solutions does not always modulate HIF-1α expression in the liver and kidney, an unmodulated HIF-1α response is beneficial in cases of anemia, as erythropoietin production remains unchanged, while vascular tone is adjusted (9). Differences in HIF-1α expression between organs can provide tolerance against hemorrhagic shock. Centralization of circulating blood and tolerance of acute isovolemic anemia (16) provide protection against moderate hemorrhage.

Tissue hypoperfusion and vasoconstriction followed by acute hemorrhagic shock can lead to tissue hypoxia. Acute hypoxia stimulates the expression of HIF-1α and p38 mitogen-activated protein kinase (MAPK), particularly in the lung, which are linked to the proliferation of pulmonary artery fibroblasts and remodeling (30). Pulmonary and systemic vasoconstriction and low peripheral perfusion are associated with use of a modified Hb tetrametric solution (11, 22), which causes scavenging of nitric oxide (NO) and enhanced endothelin release (10). NO scavenging enhances hypoxic pulmonary vasoconstriction (1), worsens pulmonary hypertension and reduces cardiac output after hemorrhagic shock. In the present study, HIF-1α expression, a marker of hypoxia, did not increase following HbV resuscitation compared to LR resuscitation. This suggests that HbV does not increase NO scavenging or impede microcirculation based on an endothelial cell disorder (23). A definitive difference is seen with the use of HBOCs that induce vasoconstriction (11). For instance, blood lactate concentration decreased following resuscitation with HbV.

Injury, hemorrhagic shock and fluid resuscitation can produce an inflammatory response such as postinjury ARDS, an acute inflammation of the lungs (17). Our results suggest that inflammation of the lungs, as measured by TNF-α and HIF-1α expression, far exceeded that of other organs. LR resuscitation was shown to produce a smaller hemorrhagic shock effect in the lung than the equivalent volume of normal saline (29). It is, therefore, of clinical interest that in the present study there were no significant differences between HbV and LR resuscitation groups in the extent of inflammation in the lung or other organs.

The key cellular mediators in the pathogenesis of proinflammatory effects are neutrophil polymorphonuclear leucocytes (PMN) (3, 4) and endothelial cells (15). PMNs are primed by plasma from stored RBCs; and the older the RBCs, the greater the priming effect (21). To reduce the induction of cytokines following RBC transfusion, PMNs can undergo prestorage leukoreduction treatment (2, 7, 12). However this does not eliminate all inflammatory reactions. The use of RBC substitutes may overcome the problems of inflammatory reactions. However, in future studies it will be important to demonstrate that, in critical situations, fewer inflammatory reactions are induced by artificial oxygen carriers than by RBCs.

In conclusion, we demonstrated that fluid resuscitation with HbV solution for moderate hemorrhagic shock did not influence the expression of HIF-1α and TNF-α mRNA in the heart, lung, kidney, liver and spleen compared with fluid resuscitation using LR solution, despite blood lactate concentrations changing after fluid resuscitation. Inflammation of the lung was significantly greater than that of other organs after hemorrhagic shock and fluid resuscitation, but the extent of inflammation did not differ according to the type of fluid resuscitation.

Acknowledgements

This research was supported by a Health and Labour Sciences Research Grant for Research on Regulatory Science of Pharmaceuticals and Medical Devices, from the Ministry of Health, Labour and Welfare, Japan.

REFERENCES

1. Biarent D, Hubloue I, Bejjani G, Melot C, Jespers P, Naeije R and Leeman M (2006) Role of endothelins and nitric oxide in the pulmonary circulation of perinatal lambs during hyperoxia and hypoxia. *Pediatr Res* **59**, 131–136.
2. Biffl WL, Moore EE, Offner PJ, Ciesla DJ, Gonzalez RJ and Silliman CC (2001) Plasma from aged stored red blood cells delays neutrophil apoptosis and primes for cytotoxicity-abrogation by poststorage washing but not prestorage leukoreduction. *J Trauma* **50**, 426–431.
3. Biffl WL, Moore EE, Zallen G, Johnson JL, Gabriel J, Offner PJ and Silliman CC (1999) Neutrophils are primed for cytotoxicity and resist apoptosis in injured patients at risk for multiple organ failure. *Surgery* **126**, 198–202.
4. Botha AJ, Moore FA, Moore EE, Kim FJ, Banerjee A and Peterson VM (1995) Postinjury neutrophil priming and activation: an early vulnerable window. *Surgery* **118**, 358–365.

5. Boura C, Caron A, Longrois D, Mertes PM, Labrude P and Menu P (2003) Volume expansion with modified hemoglobin solution, colloids, or crystalloid after hemorrhagic shock in rabbits: effects in skeletal muscle oxygen pressure and use versus arterial blood velocity and resistance. *Shock* **19**, 176–182.
6. Chomczynski P (1993) A reagent for the single-step simultaneous isolation of RNA, DNA and proteins from cell and tissue samples. *Biotechniques* **15**, 532–534, 536–537.
7. Dalen T, Bengtsson A, Brorsson B and Engstrom KG (2003) Inflammatory mediators in autotransfusion drain blood after knee arthroplasty, with and without leucocyte reduction. *Vox Sang* **85**, 31–39.
8. Dong F, Hall CH, Golech SA, Philbin NB, Rice JP, Gurney J, Arnaud FG, Hammett M, Ma X, Flournoy WS, Hong J, Kaplan LJ, Pearce LB, McGwin G, Ahlers S, McCarron R and Freilich D (2006) Immune effects of resuscitation with HBOC-201, a hemoglobin-based oxygen carrier, in swine with moderately severe hemorrhagic shock from controlled hemorrhage. *Shock* **25**, 50–55.
9. Eckardt KU and Kurtz A (2005) Regulation of erythropoietin production. *Eur J Clin Invest* **35**, 13–19.
10. Gulati A, Sen AP, Sharma AC and Singh G (1997) Role of ET and NO in resuscitative effect of diaspirin cross-linked hemoglobin after hemorrhage in rat. *Am J Physiol* **273**, H827–H836.
11. Hess JR, MacDonald VW and Brinkley WW (1993) Systemic and pulmonary hypertension after resuscitation with cell-free hemoglobin. *J Appl Physiol* **74**, 1769–1778.
12. Hyllner M, Tylman M, Bengtson JP, Rydberg L and Bengtsson A (2004) Complement activation in prestorage leucocyte-filtered plasma. *Transfus Med* **14**, 45–52.
13. Johnson JL, Moore EE, Offner PJ, Patrick DA, Tamura DY, Zallen G and Silliman CC (2004) Resuscitation with a blood substitute abrogates pathologic postinjury neutrophil cytotoxic function. *J Trauma* **50**, 449–456.
14. Koury J, Deitch EA, Homma H, Abungu B, Gangurde P, Condon MR, Lu Q, Xu DZ and Feinman R (2004) Persistent HIF-1alpha activation in gut ischemia/reparfusion injury: potential role of bacteria and lipopolysaccharide. *Shock* **22**, 270–277.
15. Luk CS, Gray-Statchuk LA, Capinkas G and Chin-Yee IH (2003) WBC reduction reduces storage-associated RBC adhesion to human vascular endothelial cells under conditions of continuous flow in vitro. *Transfusion* **43**, 151–156.
16. Madjdpour C, Spahn DR and Weiskopf RB (2006) Anemia and perioperative red blood cell transfusion: a matter of tolerance. *Crit Care Med* **34** (5 Suppl), S102–108.
17. Masuno T, Moore EE, Cheng AM, Moore PK, Grant AR and Johnson JL (2005) Prehospital hemoglobin-based oxygen carrier resuscitation attenuates postinjury acute lung injury. *Surgery* **138**, 335–341.
18. Moore EE, Cheng AM, Moore HB, Masuno T and Johnson JL (2006) Hemoglobin-based oxygen carriers in trauma care: scientific rationale for the US multicenter prehospital trial. *World J Surg*, [Epub ahead of print].
19. Moore EE, Johnson JL, Cheng AM, Masuno T and Banerjee A (2005) Insight from studies of blood substitutes in trauma. *Shock* **24**, 197–205.
20. Moore FA, Moore EE and Sauaia A (1997) Blood transfusion: an independent risk factor for postinjury multiple organ failure. *Arch Surg* **132**, 620–625.
21. Nielsen HJ, Reimert CM, Pedersen AM, Brunner N, Edvardsen L, Dybkjaer E, Kehlet H and Skov PS (1996) Time-dependent spontaneous release of white cell and platelet-derived bioactive substances from stored human blood. *Transfusion* **36**, 960–965.
22. Poli de Figueiredo LF, Mathru M, Solanki D, Macdonald VW, Hess J and Kramer GC (1997) Pulmonary hypertension and systemic vasoconstriction may offset the benefits of acellular hemoglobin blood substitutes. *J Trauma* **42**, 847–856.
23. Sakai H, Hara H, Yuasa M, Tsai AG, Takeoka S, Tsuchida E and Intaglietta M (2000) Molecular dimensions of Hb-based O2 carriers determine constriction of resistance arteries and hypertension. *Am J Physiol Heart Circ Physiol* **279**, H908–H915.
24. Sakai H, Horinouchi H, Masada Y, Takeoka S, Ikeda E, Takaori M, Kobayashi K and Tsuchida E (2004) Metabolism of hemoglobin-vesicles (artificial oxygen carriers) and their influence on organ functions in a rat model. *Biomateria* **25**, 4317–4325.
25. Sakai H, Masada Y, Horinouchi H, Yamamoto M, Ikeda E, Takeoka S, Kobayashi K and Tsuchida E (2004) Hemoglobin-vesicles suspended in recombinant human serum albumin for resuscitation from hemorrhagic shock in anesthetized rats. *Crit Care Med* **32**, 539–545.
26. Sakamoto A, Matsumura J, Mii S, Gotoh Y and Ogawa R (2004) A prostaglandin E2 receptor subtype EP4 agonist attenuates cardiovascular depression in endotoxin shock by inhibiting inflammatory cytokines and nitric oxide production. *Shock* **22**, 76–81.
27. Silliman CC, Moore EE, Johnson JL, Gonzalez RJ and Biffl WL (2004) Transfusion of the injured patient: proceed with caution. *Shock* **21**, 291–299.
28. Terajima K, Tsueshita T, Sakamoto A and Ogawa R (2006) Fluid resuscitation with hemoglobin vesicles in a rabbit model of acute hemorrhagic shock. *Shock* **25**, 184–189.
29. Watters JM, Brundage SI, Todd SR, Zautke NA, Stefater JA, Lam JC, Muller PJ, Malinoski D and Schreiber MA (2004) Resuscitation with lactated ringer's does not increase inflammatory response in a Swine model of uncontrolled hemorrhagic shock. *Shock* **22**, 283–287.
30. Welsh DJ, Scott PH and Peacock AJ (2006) p38 MAP kinase isoform activity and cell cycle regulators in the proliferative response of pulmonary and systemic artery fibroblasts to acute hypoxia. *Pulm Pharmacol Ther* **19**, 128–138.
31. Yoshizu A, Izumi Y, Park S, Sakai H, Takeoka S, Horinouchi H, Ikeda E, Tsuchida E and Kobayashi K (2004) Hemorrhagic shock resuscitation with an artificial oxygen carrier, hemoglobin vesicle, maintains intestinal perfusion and suppresses the increase in plasma tumor necrosis factor-alpha. *ASAIO J* **50**, 458–463.
32. Zallen G, Offner PJ, Moore EE, Blackwell J, Ciesla DJ, Gabriel J, Denny C and Silliman CC (1999) Age of transfused blood is an independent risk factor for post-injury multiple organ failure. *Am J Surg* **178**, 570–572.

Poly(ethylene glycol)-Conjugated Human Serum Albumin Including Iron Porphyrins: Surface Modification Improves the O_2-Transporting Ability

Yubin Huang,[†] Teruyuki Komatsu,[†,*] Rong-Min Wang,[†,‡] Akito Nakagawa,[†] and Eishun Tsuchida[†,*]

Advanced Research Institute for Science and Engineering, Waseda University, 3-4-1 Okubo, Shinjuku-ku, Tokyo 169-8555 Japan, and Key Laboratory of Polymer Materials of Gansu Province, Institute of Polymer, Northwest Normal University, Lanzhou 730070, China. Received November 3, 2005; Revised Manuscript Received February 10, 2006

Artificial O_2-carrying hemoprotein composed of human serum albumin including tetrakis(*o*-amidophenyl)-porphinatoiron(II) (Fe4P or Fe3P) [HSA−FeXP] has been modified by maleimide- or succinimide-terminated poly(ethylene glycol) (PEG), and the formed PEG bioconjugates have been physicochemically characterized. 2-Iminothiolane (IMT) reacted with the amino groups of Lys to create active thiol groups, which bind to α-maleimide-ω-methoxy PEG [Mw: 2-kDa (PEG_{M2}), 5-kDa (PEG_{M5})]. On the other hand, α-succinimidyl-ω-methoxy PEG [Mw: 2-kDa (PEG_{S2}), 5-kDa (PEG_{S5})] directly binds to Lys residues. MALDI-TOF MS of the PEG-conjugated HSA−FeXP showed distinct molecular ion peaks, which provide an accurate number of the PEG chains. In the case of PEG_{MY}(HSA−FeXP), the spectroscopic assay of the thiol groups also provided the mean of the binding numbers of the polymers, and the degree of the modification was controlled by the ratio of [IMT]/[HSA]. The viscosity and colloid osmotic pressures of the 2-kDa PEG conjugates (phosphate-buffered saline solution, [HSA] = 5 g dL^{-1}) were almost the same as that of the nonmodified one, whereas the 5-kDa PEG binding increased the rheological parameters. The presence of flexible polymers on the HSA surface retarded the association reaction of O_2 to FeXP and stabilized the oxygenated complex. Furthermore, PEG_{MY}(HSA−FeXP) exhibited a long circulation lifetime of FeXP in rats (13−16 h). On the basis of these results, it can be concluded that the surface modification of HSA−FeXP by PEG has improved its comprehensive O_2-transporting ability. In particular the PEG_{MY}(HSA−FeXP) solution could be a promising material for entirely synthetic O_2-carrying plasma expander as a red cell substitute.

INTRODUCTION

Poly(ethylene glycol) (PEG) is commonly used for the surface modification of peptides, proteins, enzymes, and liposome to confer several potential beneficial effects: not only a longer plasma half-life and nonimmunogenicity but also a solubility in organic solvents and extreme thermostability (*1*−*4*). To develop an artificial O_2 carrier, substantial efforts have been directed to the preparation of PEG-conjugated hemoglobin (Hb) over the past decades (*5*−*8*), and the optimized PEG−Hbs are currently being tested in clinical trials. Human serum albumin (HSA) is a versatile protein, which is found in our blood plasma at a high concentration (4−5 g dL^{-1}) (*9*). We have reported that HSA including tetrakis(*o*-amidophenyl)porphinatoiron(II) (Fe3P or Fe4P, Chart 1) [HSA−FeXP] can reversibly bind and release O_2 under physiological condition (pH 7.4, 37 °C) in a fashion similar to Hb (*10*). The administration of this synthetic O_2 carrier into anesthetized rats has proved its safety and O_2-transporting efficacy (*11*). Nevertheless, there is only one defect in that the FeXP molecule easily dissociates from HSA when infused into animals. This is due to the fact that FeXP is noncovalently bound to the hydrophobic cavity of albumin with binding constants (K) of 10^4−10^6 (M^{-1}). Natural heme, namely protoporphinatoiron IX, is also incorporated into HSA and shows a 10^2−10^4-fold higher K compared to FeXP (*12*); however, it is released from HSA during blood circulation with a half-life of 2.5−3.6 h (*13*, *14*). Under these circumstances, we postulated that the surface modification of HSA−FeXP by PEG could help to prolong the circulation life of FeXP and thereby retain its O_2-transporting ability for a long period. Although HSA is a very common plasma protein, its PEG conjugation chemistry has not yet been studied in detail. It is known that a huge variety of drugs are incorporated into specific sites of HSA (*9*). The PEG modification should prevent the rapid release of these drugs from the HSA scaffold and contribute to raising their potential therapeutic efficacies.

Chart 1. Structures of O_2-Adduct Complexes of Tetrakis-(*o*-amidophenyl)porphinatoiron(II)

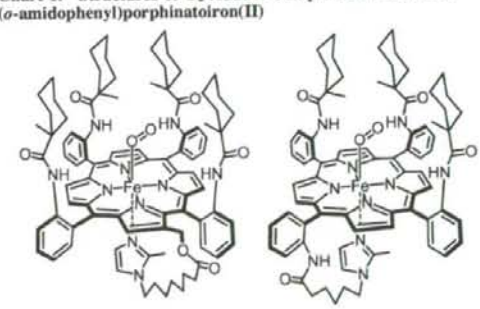

Fe4P Fe3P

In the present study, we have systematically prepared several PEG-conjugated HSA−FeXPs and characterized their physicochemical properties. The surface modification by PEG affects the viscosity and colloid osmotic pressure of the solution, O_2-binding behavior of the parent HSA−FeXP, and circulatory lifetime of FeXP. The PEG-conjugated HSA−FeXP could be

* Corresponding authors: (E.T.) Tel: +81-3-5286-3120, Fax: +81-3-3205-4740, E-mail: eishun@waseda.jp. (T.K.) E-mail: teruyuki@waseda.jp; eishun@waseda.jp.

† Waseda University.

‡ Northwest Normal University.

10.1021/bc050315+ CCC: $33.50
Published on Web 02/22/2006

of extreme medical importance as a red cell substitute or O_2-therapeutic reagent.

EXPERIMENTAL PROCEDURES

Materials and Apparatus. All reagents were purchased from commercial sources as special grades and used without further purification. 2-Iminothiolane hydrochloride (IMT) was purchased from Wako Pure Chemical Industries, Ltd. (Osaka, Japan). α-[3-(3-Maleimido-1-oxopropyl)amino]propyl-ω-methoxy PEG [averaged Mw: 2333 (Sunbright ME-020MA, PEG_{M2}), averaged Mw: 5207 (Sunbright MEMAL-50H, PEG_{M5})] and α-succinimidyloxyglutaryl-ω-methoxy PEG [averaged Mw: 2325 (Sunbright MEGC-20HS, PEG_{S2}), averaged Mw: 5261 (Sunbright MEGC-50HS, PEG_{S5})] were purchased from NOF Corp. (Tokyo, Japan). 2-{8-(2-Methylimidazolyl-1-yl)-octanoyloxymethyl}-5,10,15,20-tetrakis{α,α,α,α-*o*-(1-methylcyclohexanamido)phenyl}porphinatoiron(III) chloride (Fe4P) and 5,10,15-tris{α,α,α-*o*-(1-methylcyclohexanamido)-phenyl}-20-mono-[β-*o*-{6-(2-methylimidazolyl) hexanamido}-phenyl]porphinatoiron(III) chloride (Fe3P) were synthesized using previously reported procedures (*10d,e*). Recombinant HSA was provided by the NIPRO Corp. (Osaka, Japan). The UV−vis absorption spectra were recorded using an Agilent 8453 UV−visible spectrophotometer fitted with an Agilent 89090A temperature control unit. The water was deionized using Millipore Elix and Simpli Lab-UV.

Preparation of PEG-Conjugated HSA−FeXP. The HSA−FeXP solutions ($X = 3, 4$, [HSA]: 5 g dL^{-1}, [FeXP]/[HSA]= 4 (mol/mol), pH 7.4) were prepared as described elsewhere (*10b,d*).

PEG_{MY}(HSA−FeXP): The modification of HSA−FeXP by α-maleimide-ω-methoxy PEG_{M2} was, for instance, carried out as follows. IMT (72 mg, 0.54 mmol) was slowly added to the HSA−FeXP solution (48 mL, [HSA]: 5 g dL^{-1}, [Fe4P] = 3 mM, pH 7.4) ([IMT]/[HSA] = 15/1, mol/mol) and gently stirred at room temperature in the dark. After 3 h, PEG_{M2} (1.44 g, $[PEG_{M2}]$/[HSA]:20/1, mol/mol) was added to the mixture, which was continually stirred for another 2 h. The resultant solution was ultrafiltered and washed by at least a 600 mL of phosphate-buffered saline (PBS) solution (pH 7.4) to remove any unreacted IMT and PEG_{M2} using the ADVANTEC UHP-76K holder with a Q0500 076E membrane (cutoff Mw: 50 kDa). The volume was finally condensed to 48 mL and sterilized by a DISMIC 0.45 μm filter, producing the PEG_{M2}(HSA−FeXP) solution. The FeXP concentration was determined by the assay of the iron ion by inductively coupled plasma (ICP) spectrometry using a Seiko Instruments SPS 7000A Spectrometer. The HSA concentration was calculated from the intensity of the circular dichroism spectrum at 208 nm, because the molar ellipticity of HSA (1.9×10^4 deg cm^2 $dmol^{-1}$) was unaltered after the PEG conjugation. Circular dichroism (CD) spectra were obtained using a JASCO J-725 spectropolarimeter. The concentration of the HSA sample was 0.15 μM in PBS, and quartz cuvettes with a 10-mm thickness were used for the measurements over the range of 195−250 nm. The PEG_{M2}(HSA−Fe3P) and PEG_{M5}-(HSA−Fe4P) solutions were also prepared by the same procedure. The product was sealed in a glass bottle under CO pressure and stored at 4 °C.

PEG_{SY}(HSA−Fe4P): The surface modification of HSA−Fe4P by α-succinimidyl-ω-methoxy PEG_{S2} was carried out as follows. PEG_{S2} (0.72 g, 0.36 mmol) was directly added to the HSA−Fe4P solution ([HSA]: 5 g dL^{-1}, [Fe4P] = 3 mM, pH 7.4) ($[PEG_{S2}]$/[HSA]:10/1, mol/mol), and the mixture was stirred at room temperature for 2 h. The resultant solution was ultrafiltered, condensed (48 mL), and sterilized as described above, producing the PEG_{S2}(HSA−Fe4P) solution. Using PEG_{S5} instead of PEG_{S2}, PEG_{S5}(HSA− Fe4P) was obtained. The Fe4P and HSA concentrations were determined by the same procedures for PEG_{MY}(HSA−FeXP).

Matrix-Associated Laser Desorption Ionization Time-of-Flight Mass Spectra (MALDI-TOF MS). The MALDI-TOF MS were obtained using a Shimadzu/Kratos AXIMA-CFR S/W Version 2, which was calibrated by BSA (Sigma A-0281) and HSA (Sigma A-3782). The specimens were prepared by mixing the aqueous sample solution (10 μM, 1 μL) and matrix (10 mg mL^{-1} sinapinic acid in 40% aqueous CH_3CN, 1 μL) on the measuring plate and air-drying.

Determination of Mean of PEG_{MY} Chains per Protein by Assay of Thiol Groups. The active thiol groups on the protein surface can be assayed by the disulfide exchange reaction with 2,2′-dithiopyridine (2,2′-DTP) to produce 2-thiopyridinone (2-TP) with an absorption at 343 nm (molar absorption coefficient (ϵ_{343}): 8.1×10^3 M^{-1} cm^{-1}) (*15*). Quantitative spectroscopic measurements conveniently provide the thiol concentration. The parent HSA−FeXP showed a small absorption band in this range, which should be subtracted from the spectrum after the disulfide exchange reaction. The difference in the thiol groups per HSA−FeXP before and after the PEG_{MY} modification corresponds to the mean of the PEG_{MY} chains on the protein surface.

Solution Properties. The viscosity and density of the PEG-conjugated HSA−FeXP solution (PBS, pH 7.4) were obtained using an Anton Paar DSC 300 capillary viscometer at 37 °C. The colloid osmotic pressures of the solutions (PBS, pH 7.4) were measured by a WESCOR 4420 Colloid Osmometer at 25 °C. A membrane filter with a 30 kDa cutoff was used.

O_2-Binding Parameters. O_2-binding to PEG-conjugated HSA−FeXP was expressed by eq 1,

$$\mathrm{PEG(HSA-FeXP)} + \mathrm{O_2} \underset{k_{off}}{\overset{k_{on}}{\rightleftharpoons}} \mathrm{PEG(HSA-FeXPO_2)} \quad (1)$$

where $K = k_{on}/k_{off}$. The O_2-binding affinity (gaseous pressure at half O_2 binding for FeXP, $P_{1/2} = 1/K$) was determined by spectral changes at various partial pressures of O_2/N_2 as previously reported (*10b,d*). The FeXP concentrations of 10−20 μM were normally used for the UV−vis absorption spectroscopy. The spectra were recorded within the range of 350−700 nm. The half-lifetime of the O_2-adduct complex was determined by the time dependence of the absorption intensity at 550 nm (O_2-adduct species). The association and dissociation rate constants for O_2 (k_{on}, k_{off}) were measured by a competitive rebinding technique using a Unisoku TSP-1000WK laser flash photolysis as reported in a previous paper (*16*).

Circulation Lifetime in Vivo. The animal investigations were carried out using twenty male Wistar rats (297 ± 29 g). All animal handling and care were in accordance with the NIH guidelines. The protocol details were approved by the Animal Care and Use Committee of Keio University. The PEG-conjugated HSA−FeXP solution (20% volume of the circulatory blood) was intravenously injected into rats from the tail vein (1 mL/min) under an inhalation anesthesia with diethyl ether ($n = 4$ each). Blood was taken from the tail vein at 3, 30 min, 1, 2, 4, 8, 16 h, 1, 2, 3 days (10 time points) after the infusion and then centrifuged to isolate the serum, which was colored brown by the presence of the sample. The animals were sacrificed after the experiments by hemorrhage. The FeXP concentration was measured by an iron ion assay using ICP spectrometry as described above.

RESULTS AND DISCUSSION

Synthesis of PEG-Conjugated HSA−FeXP. The HSA−FeXP molecules were conjugated with PEG having a terminal reactive chain-end, maleimide-PEG or succinimide-PEG, at

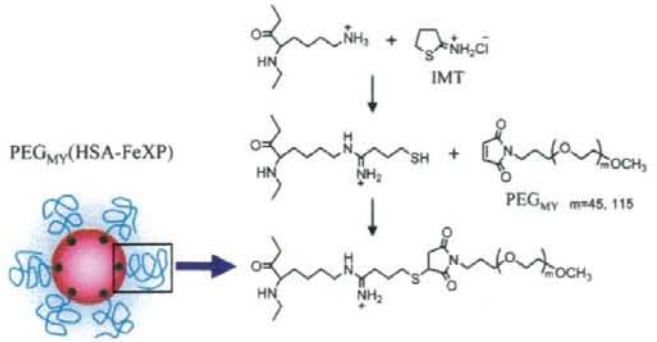

Figure 1. Two-step reaction schemes of IMT and maleimide-PEG (PEG$_{MY}$) with HSA−FeXP.

ambient temperature. Thiolation regent, IMT, quantitatively reacted with the amino groups of Lys to create active thiol groups, which bind to the α-maleimide-ω-methoxy PEG (PEG$_{M2}$ or PEG$_{M5}$) (Figure 1). The two-step reaction is reproducible and did not form any toxic side-product. On the other hand, the α-succinimidyl-ω-methoxy PEG (PEG$_{S2}$ or PEG$_{S5}$) directly binds to the amino groups of Lys. The gel permeation chromatogram (Sephacryl 200HR) of the well-washed PEG conjugate exhibited a single band, so that we did not need any further chromatographic purification.

The MALDI-TOF MS of PEG$_{M5}$(HSA−Fe4P), as prepared under the condition of [IMT]/[HSA−Fe4P] = 15/1 (mol/mol), showed five distinct ion peaks at 85, 90, 95, 101, and 106 kDa (Figure 2a). No unreacted HSA−FeXP was observed at all. The difference in each mass was 5.25 kDa, which implies that HSA−Fe4P is covalently bound to PEG$_{M5}$ and the individual peaks are attributed to PEG$_{M5}$(HSA−Fe4P) having a different number of PEG chains. Here, we have to be cautious whether these mass values involve a molecular weight of Fe4P, because our previous MALDI-TOF MS experiments of HSA−Fe4P demonstrated a single peak of HSA (Mw: 66.5 kDa); the incorporated Fe4P dissociated from the albumin during the ionization process (*10a*). In this study, we found that the mean of the surface PEG chains on HSA−FeXP is conveniently determined by a spectroscopic assay of the HSA scaffold and thiol groups. In general, the concentration of HSA is measured by the absorption at 280 nm or bromcresol green method (*17*), but they are probably obstructed by the surface modification. We then employed a CD measurement to determine the HSA concentration. The comparison of the CD spectra of HSA and PEG−HSA solutions revealed that the molecular ellipcity of albumin (ϵ_{208} = 1.9 × 10^4 deg cm^2 dmol^{-1}) is unaltered even after the PEG binding. Moreover, the presence of FeXP does not disturb the CD in the range of 190−250 nm. Therefore, the HSA concentration of PEG modified HSA−FeXP was quantitatively determined by its CD intensity at 208 nm. On the other hand, the active thiol groups on proteins are generally assayed by a disulfide exchange reaction with 2,2′-DTP (*15*). The combination of these two methodologies allows us to estimate the number of thiols on HSA−FeXP. The mean of the thiol groups was 6.7 per protein after the thiolation by IMT ([IMT]/[HSA−Fe4P] = 15 mol/mol) and decreased to 0.6 after the reaction with 20-fold excess moles of PEG$_{M5}$ (Table 1). These results suggested that the mean of 6.1 reactive thiols was conjugated with PEG$_{M5}$. The averaged molecular weight of this PEG$_{M5}$(HSA−FeXP) calculated from the intensity of the MS peak was 95 kDa. If one subtracts the total mass of the six PEG$_{M5}$ chains (5 kDa × 6 = 30 kDa) from 95 kDa, the difference of 65 kDa equals that

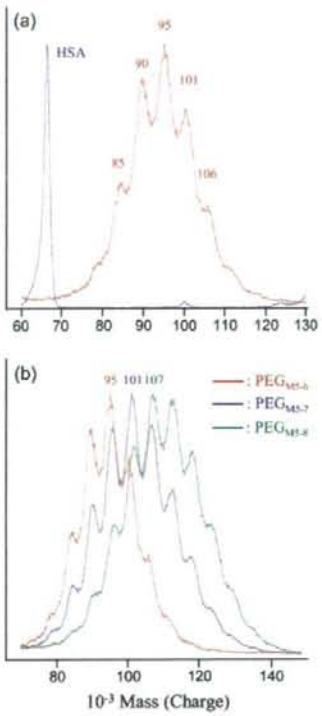

Figure 2. MALDI-TOF MS of (a) HSA and PEG$_{M5-6}$(HSA−Fe4P) and (b) PEG$_{M5}$(HSA−Fe4P) prepared in different [IMT]/[HSA−Fe4P] ratios of 15 (red), 20 (blue), and 30 (green) (mol/mol).

of HSA without Fe4P. Therefore, we concluded that all the mass ion peaks observed in the MALDI-TOF MS did not include the molecular weight of FeXP.

The number of the meleimide-PEG$_{M5}$ chains on HSA−Fe4P were modulated by the mixing ratio of [IMT]/[HSA−Fe4P] (mol/mol). The maximum peak of PEG$_{M5}$(HSA−Fe4P) in the MALDI-TOF MS significantly shifted to the higher molecular region (95 → 101 → 107 kDa) by increasing the IMT (Figure 2b). It is quite remarkable that the distributions of the entire spectral pattern were always identical. The averaged binding number of the PEG$_{M5}$ chains per HSA estimated from the intensity of the mass peak was consistent with the number determined from the assay of the thiol groups (Table 1).